

LIQUEFACTION EVALUATION OF FLY ASH TAILINGS DAM

A Thesis Submitted
in Partial Fulfilment of the Requirements
for the Degree of
MASTER OF TECHNOLOGY

by
AMIT PRANAV

to the
Department of Civil Engineering
Indian Institute of Technology, Kanpur
April, 1996

14 MAY 1996

CENTRAL
FEDERAL

Case No. A. 121510



CE-1996-M-PRA-LIQ

CERTIFICATE

*This is to certify that the present research work entitled LIQUEFACTION
EVALUATION OF FLY ASH TAILINGS DAM has been carried out by AMIT
PRANAV under my supervision and it has not been submitted elsewhere for a degree.*

Umesh Dayal

Dr. UMESH DAYAL

Professor

Dept. of Civil Engineering

Indian Institute of Technology

Kanpur

23/4/96
a

APRIL 1996

ACKNOWLEDGEMENT

The author would like to express his deep sense of gratitude to his thesis supervisor *Dr. Umesh Dayal* for his valuable guidance, inspiration, encouragement, and help throughout the present work and also his painstaking review of the manuscript

I greatly appreciate the valuable suggestions received from *Dr. Yudhbir*.

My special thanks goes to *Dr. P. K. Basudhar* and *Dr. Sarvesh Chandra* who agreed to evaluate my thesis work within a short period.

I would like to acknowledge the help and continuous support received from laboratory staffs *Mr. R. P. Trivedi*, *Mr. A.K.Srivastava*, *Mr. Gulabchand* and *Mr. Parshuram*.

Finally I would like acknowledge all my friends specially *Mr. C. Thakur*, *Satya Prakash*, *Jimmy*, *Sandeep*, *Brahmankar* and others for their constant encouragement and necessary help given by them during my whole M.Tech. programme.

amit pranas

*in
memory of
my
grand parents*

ABSTRACT

Fly ash, a waste material of the thermal power plant is being produced enormously in our country, whereas its utilization is very limited. At present it is generally disposed off near the vicinity of thermal power plant in the form of lagoon ash. In the present investigation liquefaction analysis of embankment constructed by "Upstream method of stage construction" is carried by empirical methods, pseudo static method, steady state method and simplified dynamic analysis.

In this investigation fly ash samples at Satpura thermal power plant (STPP) Sarni (M.P.) and Hansdeo Thermal Power Plant (HDTPP) Korba west (M.P.) sites were tested to establish necessary geotechnical properties required for the evaluation of liquefaction potential of fly ash disposal sites. As an example, a typical staged ash embankment consisting of five stages (total height of 80 ft. (24.3m)) has been evaluated.

(1) Empirical analysis was performed based on the earthquake severity Index (ESI) procedure as outlined by ICOLD applicable for earthquake zone of the site and typical upstream embankment configuration.

(2) Pseudo static analysis was carried out as per the Recommendation given in I.S.1893:1984.

(3) In steady state method, consolidated undrained test with pore pressure measurement were performed on samples compacted at 85 %, 90% , 95 % and 100 % Standard Procter density and on a very loose sample and the void ratio versus S_{us} relationship were established. Settled ash slurry tube samples were prepared in the laboratory at various consolidation pressure simulating the field condition and a relationship between void ratio versus

consolidation pressure was established. Octahedral stresses likely to be developed in different layers of settled ash, is computed from the applied vertical consolidation pressure on the soil surface. Corresponding to that pressure, the void ratio was determined from the tube sample results. The corresponding undrained steady state shear strength (S_{us}) values were determined from S_{us} versus void ratio relationship. Embankment stability analysis was carried out using PCSTABL5 program and it was found that the embankment is safe for five stages of upstream construction.

(4) Simplified dynamic analysis was carried out using SHAKE program. The shear wave velocity and shear modulus were determined from the standard correlation using the laboratory test results. The analysis gave a maximum vertical deformation of 1.2 inch.(3.048 cm) for STPP and 1.07 inch. (2.71 cm) for HDTPP embankment site whereas the empirical relationship gave the vertical deformation in the range of 1.92 inch(4.88 cm.) to 0.58 inch (1.47 cm).

CONTENTS

	PAGE
TITLE	i
CERTIFICATE	ii
ACKNOWLEDGEMENT	iii
ABSTRACT	v
LIST OF FIGURES	x
LIST OF TABLES	xiii
LIST OF SYMBOLS	xiv

1.	INTRODUCTION	1
2.	LITERATURE REVIEW	4
2.1	GENERAL	4
2.2	MATERIALS SUSCEPTIBLE TO LIQUEFACTION	4
2.3	ANALYSIS OF COMPACTED EMBANKMENT	7
2.3.1	PSEUDO STATIC METHOD	7
2.3.2	DEFORMATION APPROACH	8
2.4	ANALYSIS OF UNCOMPACTED EMBANKMENT	8
2.4.1	EMPIRICAL APPROACH	9
2.4.1.1	PERFORMANCE OF EMBANKMENT DAM	9
2.4.2	PSEUDO STATIC METHOD	10
2.4.2.1	CONVENTIONAL PSEUDO STATIC METHOD	10
2.4.2.2	MODIFIED PSEUDO STATIC METHOD	12
2.4.3	STEADY STATE METHOD	12
2.4.3.1	STEADY STATE LINE	13
2.4.3.2	LIQUEFACTION EVALUATION PROCEDURE	13
2.4.3.3	DETERMINATION OF IN SITU VOID RATIO	13
2.4.3.4	DETERMINATION OF STEADY STATE VOID RATIO AS A FUNCTION OF EFFECTIVE STRESS	14

2.4.3.6	CORRECTION OF MEASURED UNDRAINED STEADY STATE STRENGTH TO IN SITU VOID RATIO	19
2.4.3.7	DETERMINATION IN SITU DRIVING SHEAR STRESS AND THE FACTOR OF SAFETY	19
2.4.4	SIMPLIFIED DYNAMIC ANALYSIS	22
2.4.4.1	ESTIMATING DAM AND EMBANKMENT EARTHQUAKE INDUCED DEFORMATION	22
2.4.4.2	DETERMINATION OF YIELD ACCELERATION	23
2.4.3.3	DETERMINATION OF EARTHQUAKE INDUCED ACCELERATION	23
2.4.5	COMPLETE DYNAMIC ANALYSIS	27
2.4.5.1	DETERMINE THE PREEARTHQUAKE STATIC STRESS IN THE EMBANKMENT	27
2.4.5.2	DETERMINE THE DYNAMIC RESPONSE OF THE EMBANKMENT AND FOUNDATION TO THE BASE ROCK MOTION	27
2.4.5.3	EVALUATE THE DYNAMIC SOIL BEHAVIOUR	28
2.4.5.4	EVALUATE EMBANKMENT STABILITY	28
2.5	PACKAGES USED	29
2.5.1	PCSTABL5	29
2.5.2	SHAKE	30
3	EXPERIMENTAL DETAILS	33
3.1	GENERAL	33
3.2	SOURCE OF MATERIAL	33
3.3	PROPERTIES OF FLY ASH	33
3.4	Sus TEST	38
3.4.1	TEST SAMPLE	38
3.5	TEST RESULTS	40

4	THEORETICAL ANALYSIS	61
4.1	GENERAL	61
4.2	DETERMINATION OF STEADY STATE STRENGTH AT DIFFERENT DEPTH	61
4.3	DETERMINATION OF SHEAR MODULUS AND SHEAR WAVE VELOCITY AT DIFFERENT DEPTH	63
5	RESULTS AND DISCUSSION	67
5.1	GENERAL	67
5.2	ASH EMBANKMENT DETAILS	67
5.3	LIQUEFACTION ANALYSIS	69
5.3.1	EMPIRICAL APPROACH	69
5.3.2	PSEUDO STATIC ANALYSIS	73
5.3.3	STEADY STATE METHOD	74
5.3.4	SIMPLIFIED DYNAMIC ANALYSIS	74
6	CONCLUSIONS AND RECOMMENDATIONS	78
	APPENDIX I	81
	APPENDIX II	90
	REFERENCES	93

LIST OF FIGURES

FIGURE NO.	DESCRIPTION	PAGE
1.1	DIFFERENT METHODS OF STAGE CONSTRUCTION	3
2.1.A	EMPIRICAL RELATION BETWEEN EARTHQUAKE SEVERITY INDEX AND CREST SETTLEMENT	11
2.1.B	EMPIRICAL RELATION BETWEEN EARTHQUAKE SEVERITY INDEX AND HORIZONTAL CREST MOVEMENT	11
2.2	STEADY STATE LINE FOR CLEAN SAND	15
2.3	STEADY STATE LINE DETERMINED FROM SIX CONSOLIDATED UNDRAINED TESTS ON COMPACTED SPECIMENS	15
2.4	STEADY STATE POINTS FROM UNCONSOLIDATED UNDRAINED TESTS AT HIGH PRESSURE ON "UNDISTURBED SAMPLES"	17
2.5	PLOT OF DATA FOR ONE UNDRAINED TEST	20
2.6	CORRECTION OF MEASURED UNDRAINED STEADY STATE STRENGTH FOR DIFFERENCE BETWEEN IN SITU VOID RATIO AND VOID RATIO DURING TEST	21
2.7	CALCULATION OF AVERAGE ACCELERATION FROM FINITE ELEMENT RESPONSE ANALYSIS	24
2.8	VARIATION OF MAXIMUM ACCELERATION RATIO WITH DEPTH OF SLIDING MASS	26
2.9	VARIATION OF YIELD ACCELERATION WITH NORMALIZED PERMANENT DISPLACEMENT AND AVERAGE PERMANENT DISPLACEMENT	26
3.1	GRADATION CURVE FOR STPP, HDTPP AND KSTPP ASH SAMPLE	35
3.2	DEVIATOR STRESS VS. STRAIN FOR COMPACTED AND LOOSE ASH SAMPLE OF STPP	41

3.3	DEVIATOR STRESS VS. STRAIN FOR COMPACTED AND LOOSE ASH SAMPLE OFHDTTP	42
3.4	DEVIATOR STRESS VS. STRAIN FOR KSTPP COMPACTED AND LOOSE SAMPLE	43
3.5	PORE PRESSURE VS. STRAIN FOR STPP COMPACTED AND LOOSE SAMPLE	44
3.6	PORE PRESSURE VS. STRAIN FOR KSTPP COMPACTED AND LOOSE SAMPLE	45
3.7	PORE PRESSURE VS. STRAIN FOR HDTTP COMPACTED AND LOOSE SAMPLE	46
3.8	EFFECTIVE MINOR PRINCIPAL STRESS VS. STRAIN FOR STPP COMPACTED AND LOOSE SAMPLE	47
3.9	EFFECTIVE MINOR PRINCIPAL STRESS VS. STRAIN FOR KSTPP COMPACTED AND LOOSE SAMPLE	48
3.10	EFFECTIVE MINOR PRINCIPAL STRESS VS. STRAIN FOR HDTTP COMPACTED AND LOOSE SAMPLE	49
3.11	DEVIATOR STRESS VS. STRAIN FOR TUBE SAMPLES OF HDTTP FLY ASH	51
3.12	DEVIATOR STRESS VS. STRAIN FOR TUBE SAMPLES OF STPP FLY ASH	52
3.13	PORE PRESSURE VS STRAIN FOR TUBE SAMPLES OF HDTTP FLY ASH SAMPLE	53
3.14	PORE PRESSURE VS STRAIN FOR TUBE SAMPLES OF STPP FLY ASH SAMPLE	54
3.15	EFFECTIVE MINOR PRINCIPAL STRESS VS STRAIN OF TUBE SAMPLES OF HDTTP FLY ASH SAMPLE	55
3.16	EFFECTIVE MINOR PRINCIPAL STRESS VS STRAIN OF TUBE SAMPLES OF STPP FLY ASH SAMPLE	56

3.17	STEADY STATE LINE FOR STPP HDTPP AND KSTPP ASH SAMPLES	58
4.1	VOID RATIO VS CONSOLIDATION PRESSURE OF TUBE ASH SAMPLES	62
5.1	EMBANKMENT OUTLINE CONSTRUCTED BY UPSTREAM METHOD OF STAGED CONSTRUCTION	68

LIST OF TABLES

TABLE NO.	DESCRIPTION	
3.1	GEOTECHNICAL PROPERTIES ASH SAMPLES	37
3.2	VOID RATIO AND S_{us} DATA OF COMPACTED AND LOOSE FLY ASH SAMPLES	57
3.3	VOID RATIO AND S_{us} DATA OF TUBE CONSOLIDATED ASH SAMPLES	58
4.1	CALCULATION OF S_{us} SHEAR MODULUS AND SHEAR WAVE VELOCITY AT DIFFERENT DEPTH OF STPP EMBANKMENT SITE	65
4.2	CALCULATION OF S_{us} SHEAR MODULUS AND SHEAR WAVE VELOCITY AT DIFFERENT DEPTH OF HDTPP EMBANKMENT SITE	66
5.1	GEOTECHNICAL PROPERTIES OF SOIL FLY ASH SAMPLES NEEDED FOR LIQUEFACTION ANALYSIS	70
5.2	CORRELATION BETWEEN PEAK GROUND ACCELERATION AND EARTHQUAKE INTENSITY	71
5.3	DEFORMATION CALCULATION OF EMBANKMENT MADE BY HDTPP AND STPP ASH SAMPLE	72
5.4	DEFORMATION CALCULATION FOR EMBANKMENT CONSTRUCTED BY STPP AND HDTPP ASH SAMPLES	77

LIST OF SYMBOLS

A: Peak ground acceleration

B: Skempton's Pore pressure parameter

ESI: Earthquake severity Index

e: Void ratio

M: Earthquake Magnitude

q: Deviator stress

q_s : Deviator stress during steady state deformation

τ_{sus} : Undrained steady state of shear stress

τ_s : Mobilising shear stress

Δu : Pore pressure change

Δu_s : Pore pressure change during steady state deformation

ϕ : Effective friction angle

$\bar{\sigma}_3$: Effective minor principal stress

$\bar{\sigma}_{3s}$: Effective minor principal stress during steady state deformation

G: Specific Gravity

Gmax: Shear modulus

V: Shear wave Velocity

ρ : Mass density

ΔH : Vertical crest settlement

ΔD : Horizontal crest settlement

STPP: Satpura Thermal Power Plant

HDTTP: Hansdeo Thermal Power Plant

KSTTP: Korba Super Thermal Power Plant

CHAPTER 1

INTRODUCTION

In India demand of electrical energy is increasing day by day. Due to ample coal reserve in India, it has resulted in the construction of coal fired power plants. Most of the power plants being constructed or have been proposed are coal fired power plants. As a result the production of power plant waste fly ash is increasing day by day. Fly ash is a by product of those thermal power stations which are using pulverized coal as a fuel. At present 65 thermal power plants are operating in India, producing about 40 million tons of ash as a waste material in our country per annum. With the commissioning of the super power plants and increasing use of low grade coal of high ash content, the present ash production is likely to be tripled. This will pose a serious disposal and ecological problem in addition to occupying large tracts of scarce of cultivatable land.

The beneficial usage of ash in concrete ,brick making ,soil stabilization treatment and other applications have been recognized; only a small fraction of total ash produced in India is currently utilized in such applications. Until full utilization of ash is made, ash produced from the power plant will be disposed off on ground. Since the volume of ash to be disposed off is large, technical skill is essential for its disposal. It can be disposed off either by dry scheme or by wet scheme. In India ash from the most of the power plants is disposed off by wet scheme in the vicinity of the power plant as a waste material. In wet disposal scheme fly ash is generally transported as a slurry through pipe and disposed off in an impoundment (starter dyke).

When the starter dyke is approximately full four basic options are available for the disposal of ash:

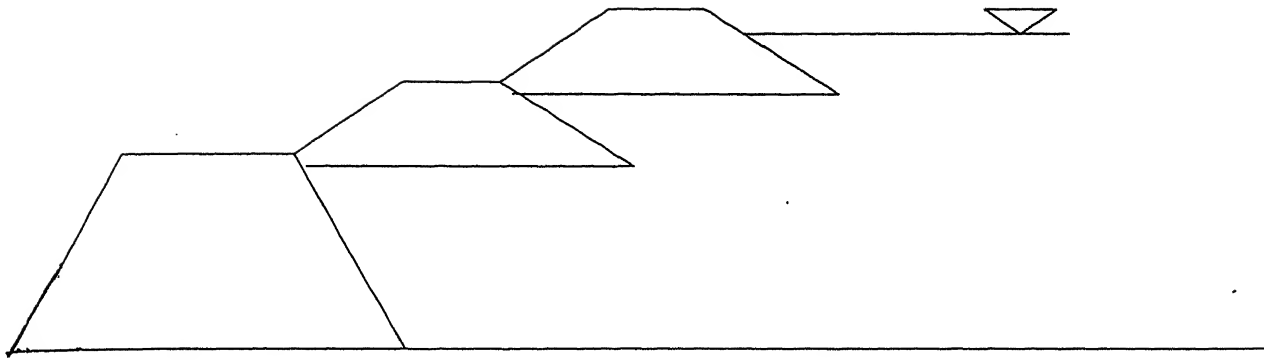
- 1) Constructing new lagoons using either conventional construction material
- 2) Having the fly ash in existing lagoons hauled to another disposal site
- 3) Raising the existing dyke using conventional material
- 4) Raising the dyke using the fly ash excavated from the lagoon.

The fourth option is considered to be very cost effective because fly ash used for constructing dyke would in addition to saving the earth filling cost, enhance the disposal capacity of the lagoon. This can be achieved by any of the following method :

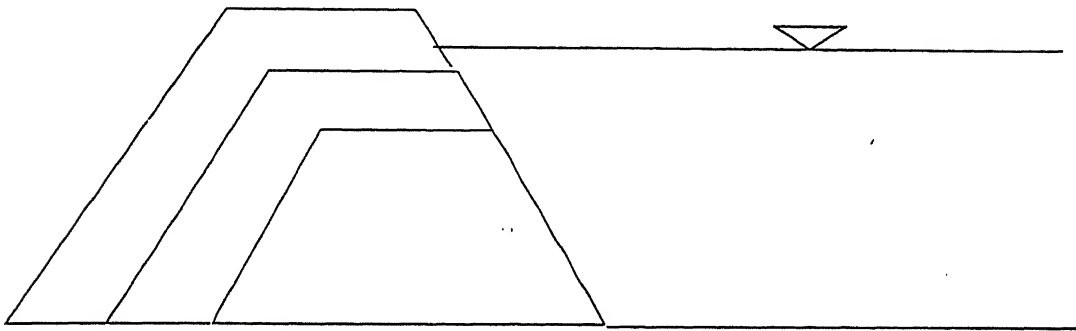
- 1) Upstream method of stage construction
- 2) Downstream method of stage construction
- 3) Centreline method of stage construction

Upstream method :

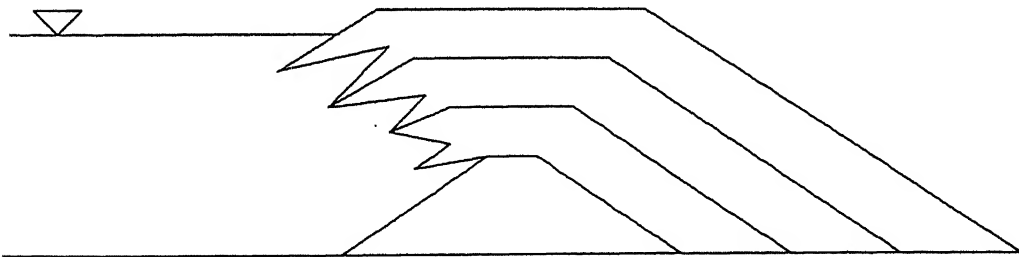
In this method an initial starter dyke is constructed at the downstream toe of proposed embankment and then embankment construction progresses upstream in stages as the height of the embankment increases. This technique requires minimum volume of structural fill for the raising dykes and it has better environmental pollution control compared to other methods because the constructed face becomes the final face of the constructed embankment. The major drawback of this method is that a part of embankment is constructed on the uncompacted ash, which is not structurally sound material. Probability of liquefaction of hydraulically filled lagoon ash is very high when it is subjected



Upstream Method of Stage Construction



Downstream Method of Stage Construction



CentreLine Method of Stage ,Construction

Fig. 1.1 : Different Methods of Stage Construction

Downstream method :

In this method, construction is carried out on the downstream side of the starter embankment so that the crest of the dam is shifted progressively towards the downstream. The main advantage of this method is that none of the embankment is constructed on the uncompacted ash as in case of the upstream method. Major drawback of this technique is that it requires relatively large volume of fill to raise the embankment.

Centreline method :

It is basically a type of downstream method in which crest of the embankment is not shifted in the downstream direction but raised vertically upward above the crest of the starter dam. This method has many design construction, environmental and operational problems and as such it is generally not adopted.

The present thesis covers the seismic design aspect of new tailings dam or fly ash embankments constructed by upstream method of staged construction.

In chapter 2 embankment stability under seismic condition has been reviewed for both compacted and uncompacted embankments. More emphasis has been given on compacted embankment constructed over the settled ash slurry.

In chapter 3 experimental setup and its result has been discussed.

In chapter 4 theoretical analysis has been carried out. Chapter 5 presents results and discussion. Conclusion and recommendation for future work has been given in chapter 6.

CHAPTER 2

LITERATURE REVIEW

2.1 General :

Liquefaction is a phenomenon where in a saturated sand and other granular materials such as fly ash loses a large percentage of shear resistance due to monotonic or cyclic loading and flows like liquid until the shear stress acting on the mass are as low as its reduced shear resistance. Earthquake causes strong reciprocating, horizontal (most damaging) and vertical forces due to inertia of the structure such as earth dam, tailing dams etc. , and the ground motions during earthquake are periodic but highly irregular. The cyclic stress reversal between compression and extension as well as repeated compressive loading tends to decrease continuously the volume of the particulate material which gives rise to increase in pore pressure .Hence the effective strength of the saturated sand decreases. The liquefaction potential and degree of liquefaction will depend on type and relative density of the sand and the average total stress as well as the level and duration of cyclic and repeated loading.

2.2 Materials Susceptible to liquefaction:

When an element of saturated soil is subjected to shaking (stimulated in laboratory by cyclic load for earthquake) the pore pressure increases. The pore pressure generated into the soil due to cyclic stress depends on a number of factors, but on the most elementary level, soil type can be considered the fundamental parameter .For saturated cohesive soils subjected to undrained cyclic loading, pore pressure is generated but usually to a limited degree. As a result the static undrained shear strength of a clay may be reduced somewhat by cyclic loading; but the soil

retains its basic integrity and liquefaction does not occur. Consequently clayey soils are not usually of primary concern in determining embankment stability under earthquake loading conditions.

Another class of material is represented by very coarse permeable deposits of cohesionless material. High permeability of such materials prevents undrained conditions from developing during cyclic shear; in effect pore pressure generated by cyclic loading dissipate as fast as they are generated. Here too liquefaction susceptibility is seldom of major concern.

Dense sand still represents another class of material. Most commonly such materials are in centreline or downstream type embankments constructed of fly ash placed in lifts and compacted under controlled conditions. Pore pressures are generated in response to undrained cyclic loading and may momentarily reach high values. However the tendency of such material to dilate quickly which reduces the pore pressure, causing the material to stabilize. Even after a large number of cyclic reversals the cumulative pore pressure is limited, although the sample may experience some degree of permanent deformation. Severe loss of strength does not occur under these conditions and therefore the compacted material does not usually experience severe seismic instability.

The most problematic class of materials consist of loose saturated sands of relative density of 30-50%. This category may apply to most upstream embankments constructed on uncompacted fly ash deposits. When it is subjected to strong and/or extended seismic shaking the undrained cyclic loading conditions is likely to occur. Pore pressures are generated during each applications of

cyclic stress reversal, and the effects become the cumulative during the duration of shaking. Under the application of uniform cycles of cyclic stress pore pressure may reach the level of the applied confining stress. At this point the effective stress within the foundation material becomes momentarily zero and initial liquefaction is said to have occurred. Following initial liquefaction, the embankment may rapidly undergo excessive strain only with a few additional cycles of stress.

Seed(1979) had reviewed the factors related to the nature of material and its depositional characteristics governs the liquefaction susceptibility. Many of those factors suggest that the liquefaction susceptibility of tailings may be greater than that of natural soil deposits at the same relative density. Those factors include grain characteristics and gradation, method of deposition, aging, previous strain history and over consolidation ratio. These factors suggest the comparison between natural soil deposits and tailings deposits at equivalent relative densities must be made with caution and that tailings samples for laboratory testing must be prepared in a way that reflects their depositional and environmental character in situ. With regards to failure of tailings dam due to ground rupture is remote and it may be possible only when the dyke is built over the actual fault zone. This type of failure is generally reviewed at the time of site selection and it shall not be, therefore, addressed here. By far the common problem in upstream method of tailings dam design is to ensure that the dyke will be stable under the anticipated levels of seismic shaking. The purpose of the literature review is to provide an overview of procedures for assessing fly ash tailings dyke stability under earthquake loading.

The technology of seismic analysis of earth dam stability is a young one. Only within last three decades the mechanism has been developed for an understanding of actual soil behaviour during earthquakes and those mechanism to conventional earth dam is not simple. In case of tailings dam, their unique material properties further complicate the problem. For a complete seismic analysis of dam /tailings dam due to earthquake loading requires (1) the estimation of seismic acceleration, (2) the response of soil/material to cyclic loading and (3) seismic analysis.

2.3 Analysis of compacted embankment :

Dams constructed of clay on clay or rock foundations have withstood extremely strong shaking under acceleration of .35 -.5 g with no permanent damage (Seed et.al. 1977, 1978). Rockfill dams have also performed well. Dams of this class are unlikely to experience failure due to seismic liquefaction. In the context of tailing embankments, they include downstream and water retention type embankments constructed of clay, rockfill, mine waste or of other material that has been well compacted under controlled conditions. For embankment of this class, seismic analysis are commonly performed using either a pseudo static or deformation approach.

2.3.1 Pseudo-static Method :

In this analysis the problem is treated as a static one, with a horizontal force applied by earthquake expressed as the product of seismic coefficient multiplied by the weight of the potential sliding mass .

Pseudo static methods have long been used and they remain most useful for seismic stability analysis in cases where cyclic liquefaction or major pore pressure build up is not anticipated.

Nevertheless, the pseudo static approach does not accurately model true embankment behaviour under major earthquake shaking. As such pseudo-static methods must be considered largely empirical in nature. However, this method is routinely used in practice for compacted embankments.

2.3.2 Deformation approach :

Deformation approach may be applied to embankment materials that do not experience severe strength reduction during application of cyclic stresses. In effect this method assumes that the embankment slope will not undergo complete failure by sliding during an earthquake but that the embankment will undergo some permanent deformation. The basis for evaluating the embankment behaviour under seismic shaking is whether or not the computed deformations lie within acceptable limits i.e. to prevent overtopping.

Procedures originally developed by Newmark(1965) have been used to estimate embankment deformation during earthquake shaking. These procedures use limiting equilibrium methods to estimate permanent displacement experienced by a rigid-body failure mass. Other simplified techniques proposed by Makadisi and Seed (1977) include consideration of the dynamic response of the embankment.

2.4 ANALYSIS OF UNCOMPACTED EMBANKMENTS :

Embankments of uncompacted material, usually unconsolidated settled fly ash, pose an entirely different analytical problem than the compacted one. In uncompacted material the pore pressure can be expected to result from strong seismic shaking, and the material can no longer be assumed to retain all or the most of its

original static strength. Upstream embankments of hydraulically discharged tailings are the most problematic variety of uncompacted embankments , but this category also includes downstream and centreline type embankments that are saturated within significant portions and are constructed of uncompacted cycloned tailings .

Many types of techniques, ranging from very crude to extremely complex, are available for seismic stability analysis of uncompacted embankments, but most suffer from their theoretical limitations or practical drawbacks. In a hierarchy of complexity, these methods include empirical evaluations, pseudo static method, in conventional or modified form, steady state method, simplified liquefaction analyses, and complete dynamic analysis.

2.4.1 EMPIRICAL APPROACH :

On the most simplistic level, it is instructive to make a preliminary assessment of seismic stability on the basis of the observed performance of hydraulic fill embankment during earthquakes .Catastrophic seismic failures or near failures of uncompacted hydraulic fill embankments have been evaluated in the context of the level of earthquake shaking they have experienced .The review of the literature suggests that most upstream embankments have survived acceleration up to about 0.15g (where g is the acceleration due to gravity).

2.4.1.1 Performance of Embankment Dams :

Behaviour of embankment dams under seismic condition include settlement, horizontal movement, cracking, pore pressure build up, slope slumping and failure, internal erosion, increase of seepage, and reservoir and impoundment breaching in the extreme cases.

The Seismic crack movement of embankment dams reflects dam

deformation associated with compression, lateral spreading and slope movements induced by earthquakes. Bureau et. al. (1985) reviewed seismic performance of earth and rock fill dams including the crest movement (settlement and horizontal movement). They introduced an Earthquake Severity Index (ESI), which reflects the influence of both the intensity and duration of the earthquake and is defined as :

$$ESI = A(M-4.5)^3 \quad \text{Eq.} \quad 2.1$$

where A = Peak ground acceleration at the dam site ;

M = Earthquake magnitude

Further an empirical relationship is given between the ESI and the crest settlement expressed as a relative settlement ratio (crest settlement divided by height). This correlation plot updated with data from Lo and Kohn is shown in Figure 2.1.a The solid line represents the interpolated trend through all the data points.

Figure 2.1.b presents a similar plot, also updated by data from Lo and Kohn (1992) correlating the horizontal relative crest movement (horizontal crest movement divided by dam height) with the Earthquake Severity Index, ESI.

2.4.2 PSEUDO STATIC METHOD :

2.4.2.1 Conventional Pseudo Static Method :

This method is also used in practice for uncompacted tailings embankments but they have even less theoretical validity than in their conventional application to compacted embankments because pore pressure due to cyclic loading are not accounted for. Failure might have been correctly predicted by using a seismic coefficient corresponding to the actual maximum acceleration experienced by the embankment during the earthquake. But there is uncertainty in

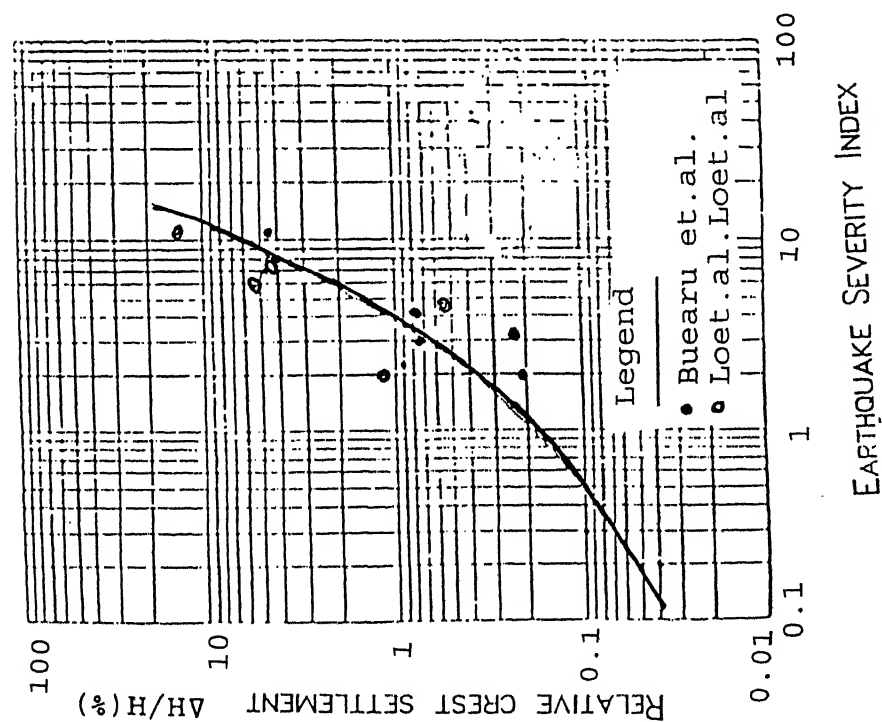


FIG. 2.1.A EMPIRICAL RELATIONSHIP BETWEEN CREST
SETTLEMENT AND EARTHQUAKE SEVERITY
INDEX (AFTER BUREAU ET.AL. 1985, LO
AND KLOHN 1992)

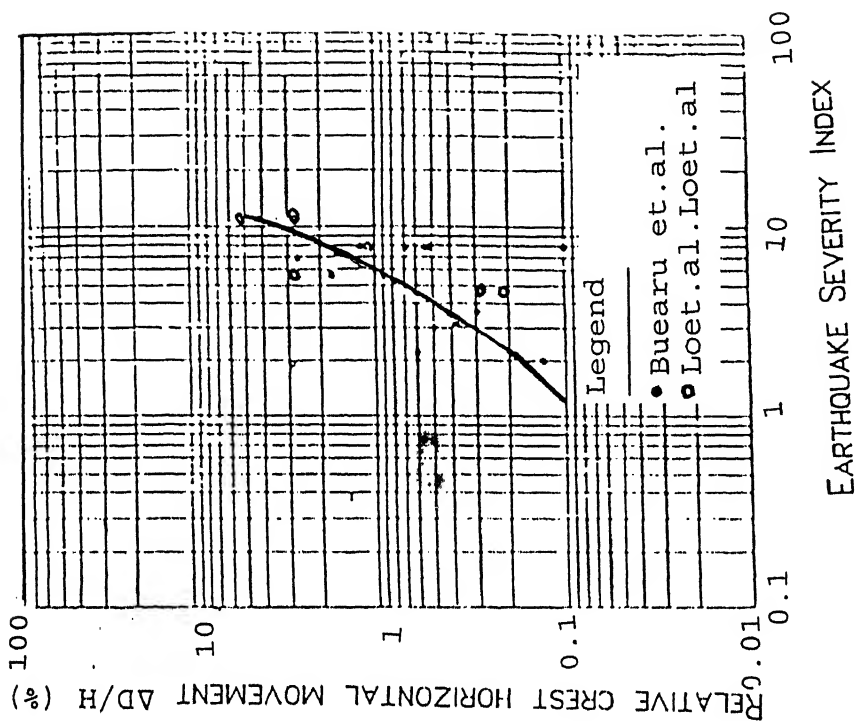


FIG. 2.1.B EMPIRICAL RELATIONSHIP BETWEEN CREST
HORIZONTAL MOVEMENT AND EARTHQUAKE
SEVERITY INDEX (AFTER BUREAU ET. AL.
1985, LO AND KLOHN 1992)

selection of appropriate strength values, hence to make a successful prediction is very rare. In general, this method can be adopted for those cases where seismic risk is so low that it can be reasonably certain that significant pore pressures due to cyclic loading will not develop. As a precaution total stress parameter may be used for saturated uncompacted material for low to moderate permeability in order to account in a crude way for pore pressures due to shear generated by the rapidly applied earthquake loading.

2.4.2.2. *Modified Pseudo Static Method :*

Several investigators have attempted to address deficiencies in the conventional pseudo static approach by accounting for pore pressures induced by cyclic shear in a more explicit way. One approach is to first consolidate the sample in the laboratory and then subject it to a number of cycles of undrained shear corresponding to the magnitude and duration of the design earthquake, and finally to shear the sample in a static undrained mode (assuming that liquefaction has not already occurred). A strength envelope results that is similar to a conventional envelope from static consolidated tests, except that the pore pressures induced by the cyclic shear are incorporated. Lee and Roth (1977) has described the use of such a strength envelope in the analysis of hydraulic fill dam.

2.4.3. *STEADY STATE METHOD :*

The steady state of deformation for any soil mass (Poulos et. al. 1985) is that state in which the mass is continuously deforming at constant volume, constant normal effective stress, constant shear stress and constant rate of shear strain. The steady state of deformation can be achieved only after the structure is completely remoulded and all particle orientation effects have

reached a steady state condition and after all particle breakage, if any is complete, so that the shear stress and the rate of deformation remain constant. The steady state can be reached in drained or undrained shear.

2.4.3.1 Steady state line

Steady state line of a soil is most commonly expressed by a best fit line plotted between void ratio vs. effective minor principal stress (on log scale) or deviator stress.

2.4.3.2. Liquefaction evaluation procedure :

Liquefaction potential in steady state method is determined by stability analysis which requires the determination of shear strength and the shear stress in situ. The shear strength used in the liquefaction analysis is the in situ undrained steady state shear strength which is difficult to determine accurately because it is very sensitive to void ratio.

Poulos et al. (1985) has recommended the detailed step wise procedure for liquefaction evaluation. The steps in the analysis related to the measurement of in situ strength are listed below :

- 1) Determination of in situ void ratio
- 2) Determination of steady state void ratio or density as a function of effective stress using compacted specimen.
- 3) Determination of undrained, steady-state strengths for undisturbed specimen.
- 4) Correction of measured undrained steady state strengths to in situ void ratio.
- 5) Calculation of in situ driving shear stress and the factor of safety against liquefaction.

2.4.3.3 Determination of in-situ void ratio :

For clays, it is relatively simple to measure in situ void

ratio using the procedure developed by Hvorslev(1949),but for sand or fly ash it is difficult to get a correct in situ void ratio. Generally fixed piston sampling, freezing of the ground and coring or block sampling in the test pit can provide satisfactory result but each one requires extra care and are not practicable for deeper strata.

It is very difficult to measure in situ void ratio accurately at depth in a bore hole ,particularly for a cohesion less soil.The in situ undrained steady state strength is highly sensitive to void ratio, therefore the in situ void ratio has to be measured with a procedure like that described in subsequent steps to obtain a suitable measurement of the undrained steady state strength(Poulos et al. 1985).

2.4.3.4. Determination of steady state void ratio as a function of effective stress using compacted sample :

A procedure is required for correcting the laboratory measured steady state strengths to the in situ void ratio because the undisturbed samples of loose sands have always lower void ratio in laboratory than in situ. Even if a sample is obtained by freezing the ground and coring, the density increases significantly during reconsolidation in the laboratory to in situ stresses. Sometimes the increase in density during consolidation is so high that it causes soil to become dilative in laboratory whereas it was contractive in situ. This means that a sample gets converted from a state in which it is in liquefiable to a state in which it is not liquefiable.

The influence of apparently minor change in void ratio on undisturbed steady state strength is shown in Figure 2.2. It shows the results of measurements of steady state strength for a clean

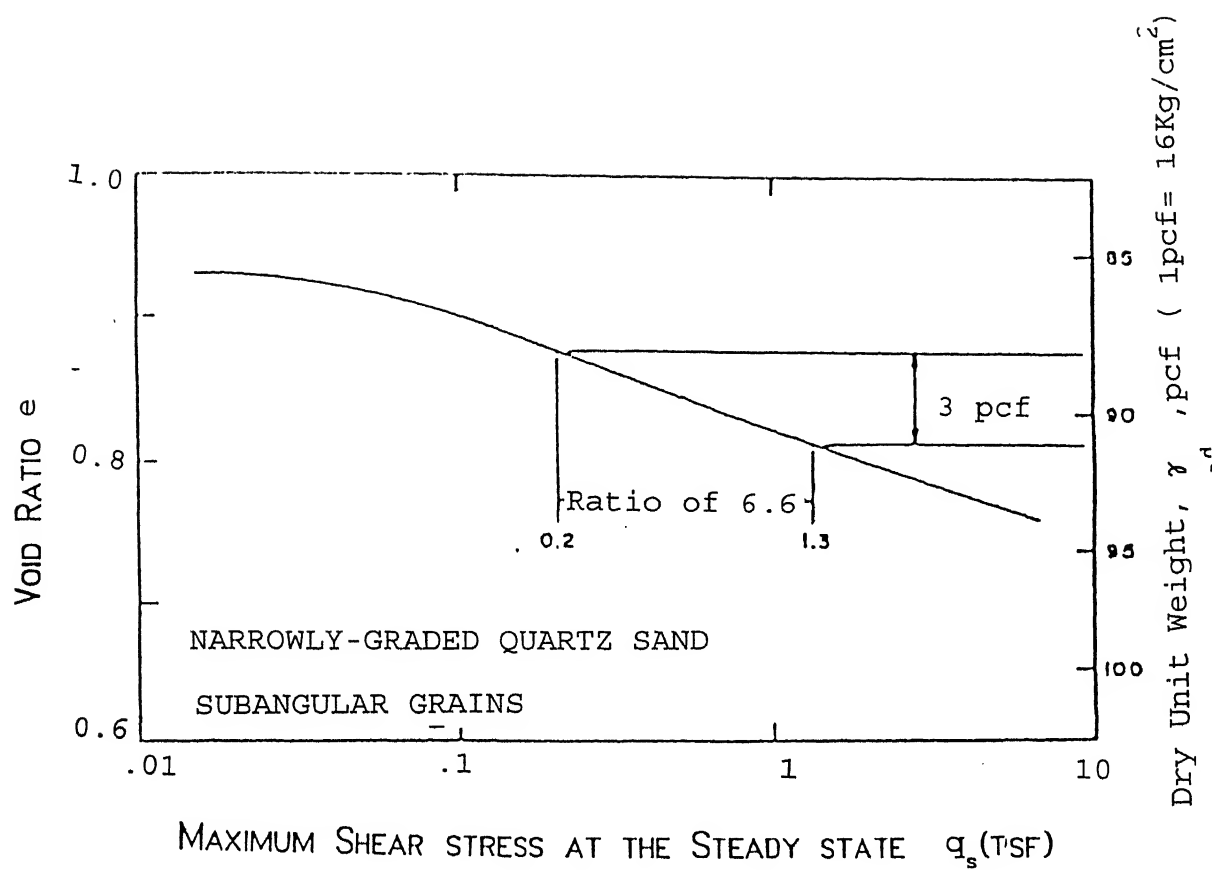


FIG.2.2 STEADY STATE LINE FOR CLEAN SAND

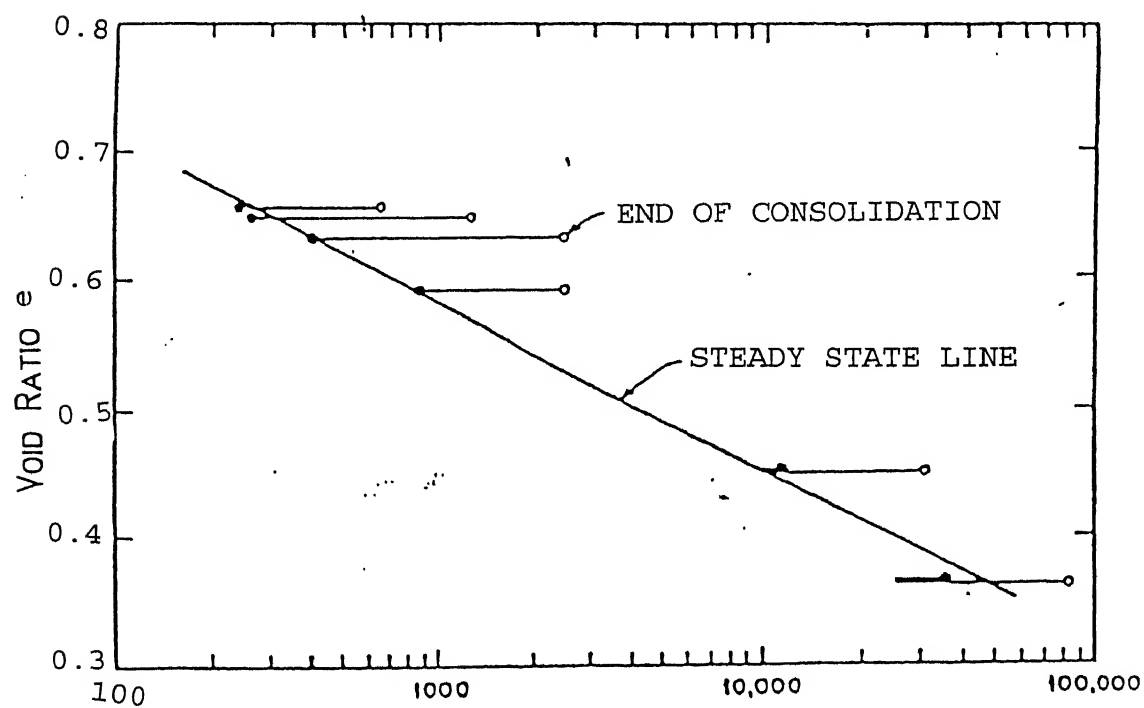
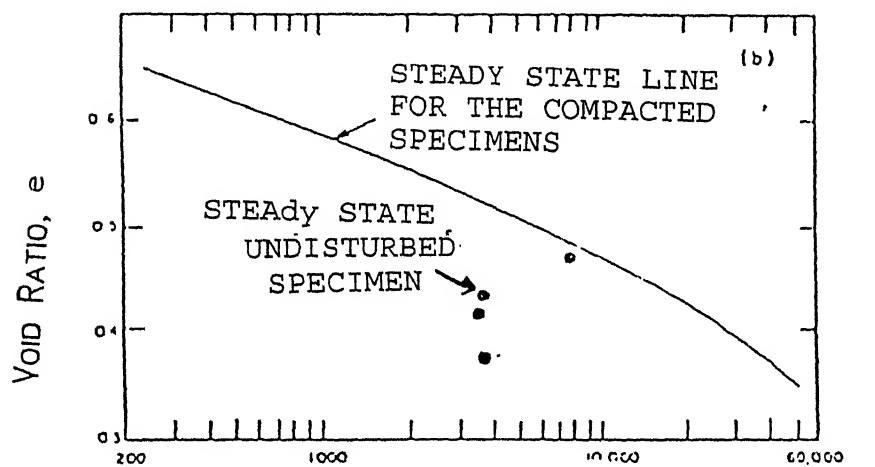
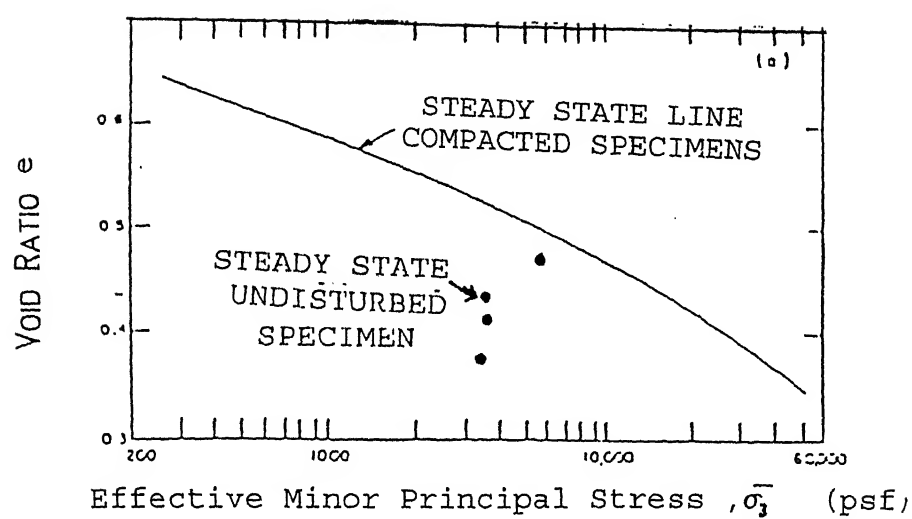


FIG. 2.3 EFFECTIVE MINOR PRINCIPAL STRESS $\bar{\sigma}_3$ (PSF)

sub angular sand, quartz and tailings sand as a function of density. As shown in this figure even a slight change in the void ratio significantly effects the S_{us} value and a correction procedure has been suggested for obtaining in situ void ratio.

The procedure for correcting laboratory measured undrained steady state strength to the in situ void ratio is based on two observations: (1) the slope of steady state line on the semi log plot is affected chiefly by the shapes of the grains in a given soil and (2) the vertical position of the steady state line is affected by even small differences in grain size distribution (Castro 1975).

The correction procedure currently used requires that the steady state line be obtained by testing five or six compacted specimens of identical soil. The soil used should be the same as that in the ground and at this stage grain shape distribution needs be well preserved, since it has the major effect on the slope of the steady state line. The results of the tests on compacted specimens are plotted on the "state diagram" (Figure 2.3) a plot of void ratio versus effective minor principal stress $\bar{\sigma}_3$. The best fit line through the points representing the steady state is the steady state line (SSL). Since it is the steady state shear strength that is needed for liquefaction analysis, it is convenient to plot the results of the undrained triaxial tests in terms of void ratio versus undrained steady state shear strength on the failure plane, S_{us} , as shown in Figure 2.4.b rather than in terms of $\bar{\sigma}_{3s}$ as shown in Figure 2.4 a. The S_{us} from the results of each consolidated undrained triaxial is computed test using the following equation :



UNDRAINED STEADY STATE SHEAR STRENGTH S_{US} (PSF)

FIG.2.4 STEADY STATE POINTS FROM UNCONSOLIDATED UNDRAINED TEST AT
HIGH PRESSURE ON UNDISTURBED SAMPLES

$$S_{us} = q_s \cos \phi_s \quad \text{Eq. 2.2}$$

$$\sin \phi_s = \frac{q_s}{\bar{\sigma}_{3s} + q_s} = \frac{q_s}{(\bar{\sigma}_{3c} - \Delta u_s) + q_s} \quad \text{Eq. 2.3}$$

$$q_s = \frac{\bar{\sigma}_{1s} - \bar{\sigma}_{3s}}{2} \quad \text{Eq. 2.4}$$

in which $\bar{\sigma}_{1s} - \bar{\sigma}_{3s}$ = Principal stress difference

$\bar{\sigma}_{3s}$ = Effective minor principal stress at the steady state

$\bar{\sigma}_{3c}$ = Effective minor principal stress at start of shear

Δu_s = Pore pressure induced in the test specimen at the steady state of deformation.

ϕ_s = Steady state friction angle

The quantities q_s , $\bar{\sigma}_{3c}$ and Δu_s are obtained directly during triaxial tests.

The steady state line obtained from the compacted samples is used to correct the strengths of "undisturbed" samples, determined in the following steps.

2.4.3.5 Determination of undrained steady state strengths for undisturbed samples :

A series of consolidated undrained triaxial test is performed on "undisturbed" samples to determine the average steady state strength. It is best to insure that the sample is contractive in nature. One procedure that can be used is to consolidate the undisturbed specimens to high effective stress, but not so high that the correction needed in section 2.4.3.6 becomes excessive. Steady state can still be determined at lower effective stress but the accuracy of the measurement is poorer than the contractive samples. Soils having some plasticity, other tests must be used to determine the steady state line, such as rotation shear test and vane shear test.

The steady state point (point s in Fig. 2.5)for each undisturbed sample is plotted on the same steady state diagram ,as shown in Fig. 2.4.a or 2.4.b with the steady state line for compacted specimen. The vertical distance between the individual point and the steady state line for compacted specimen is assumed to be due chiefly to minor differences in grain size distribution. The undrained steady state strengths shown in Fig.2.3.were obtained at the void ratio after consolidation ,not at the in situ void ratio.therefore correction of the results to the in situ void ratio must be made as described in the next steps.

2.4.3.6 Correction of measured undrained steady state strengths to in situ void ratio :

In situ void ratio is measured during taking out the "undisturbed" samples .Using the void ratio of undisturbed samples measured in laboratory after consolidation, it is joined with the in situ void ratio keeping this line parallel to the steady state line of the compacted samples on the state diagram.The estimated in situ undrained steady state strength is selected from the abscissa, as shown in Fig.2.6 .

2.4.3.7 Determination of in situ driving shear stress and the factor of safety :

The in situ driving shear stress in the zone being evaluated is calculated by conventional methods of stability analysis.It is the minimum shear stress that is required to maintain the static equilibrium.The shear stress along the potential failure surface in the zone being evaluated can be computed using limiting equilibrium approaches, such as method of the slices, circular arc type ,wedge type or by using a non circular surface .One can make

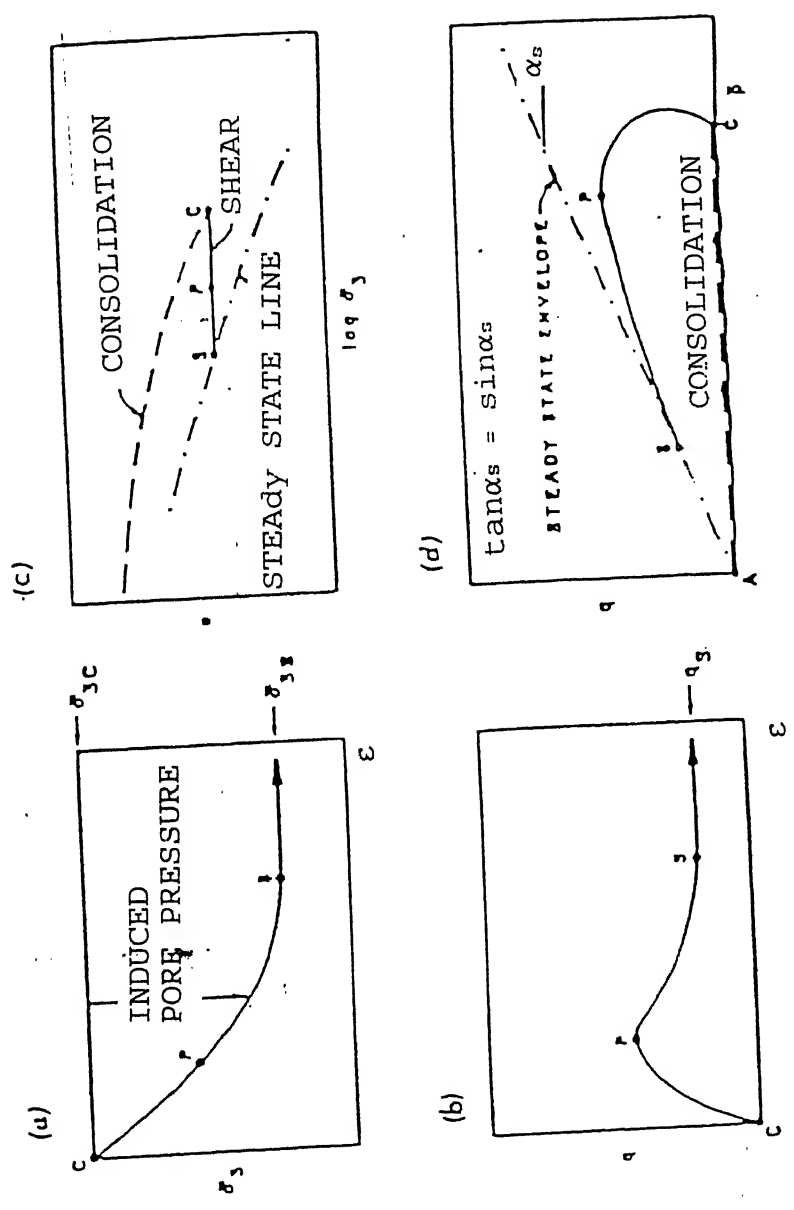


FIG 2.5 PLOT OF DATA FOR ONE UNDRAINED TEST ON CONTRACTIVE SPECIMEN TO DETERMINE STEADY STATE STRENGTH (SCHEMATIC)

A) EFFECTIVE STRESS (B) STATE (C) STRESS STRAIN (D) STRESS PATH

(AFTER POULOS ET. AL. 1985)

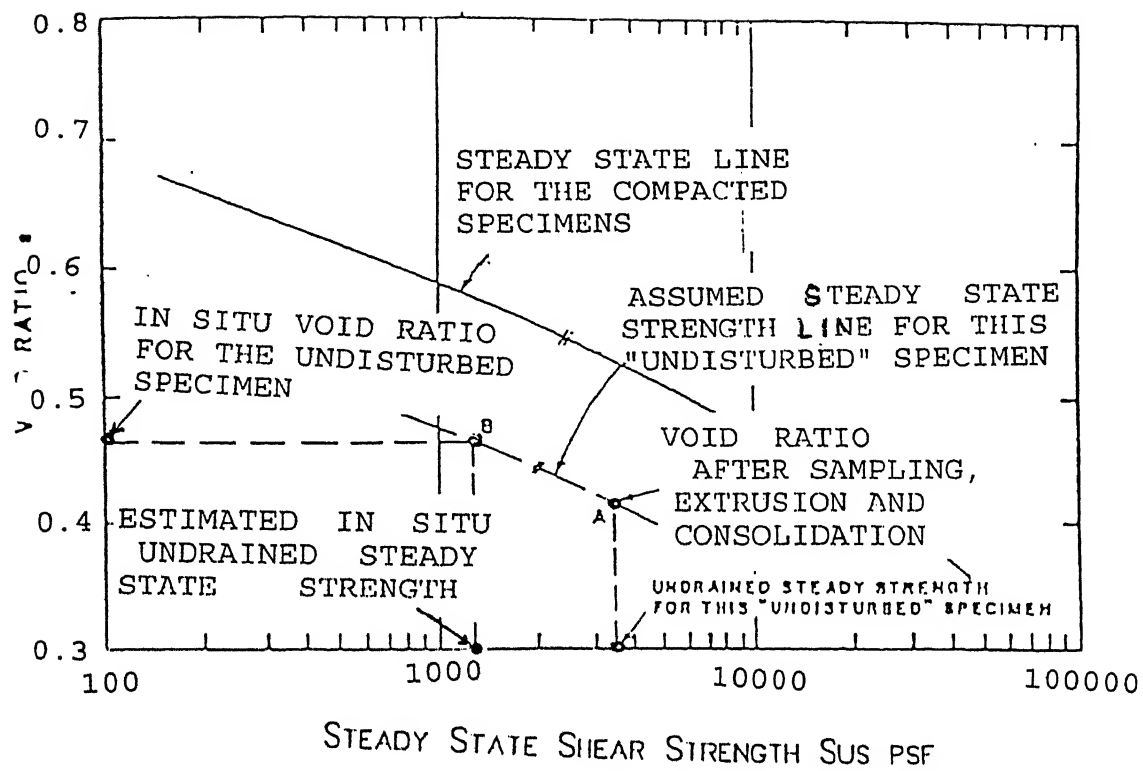


FIG. 2.6 CORRECTION OF MEASURED UNDRAINED STEADY STATE STRENGTH FOR DIFFERENCE BETWEEN IN SITU VOID RATIO DURING TEST

type ,wedge type or by using a non circular surface .One can make an assumption about the distribution of stresses along the failure surfaces to calculate this shear stress.

Using the stability analysis , the driving shear stress " τ_d " is computed.If its average value is less than the undisturbed steady state shear strength in all zones along trial failure surface ,then liquefaction cannot occur.

The factor of safety against liquefaction F_L , is given by

$$F_L = \frac{\text{Undrained steady state shear strength}}{\text{Shear stress required to maintain static equilibrium}}$$

The undrained steady state strength calculated above is the minimum strength that a contractive soil mass can have at the void ratio in situ.Therefore the factor of safety need only be sufficiently greater than 1 to ensure that any uncertainty in the void ratio is accounted for.

2.4.4 Simplified Dynamic analysis:

2.4.4.1 Estimating Dam And Embankment Earthquake Induced Deformation :

A simple yet rational approach to the design of dam and embankment under earthquake loading is based on the concept of permanent deformation as proposed by Newmark(1965) but modified to allow for the dynamic response of the dam and embankment as proposed by Seed and Martin (1966) rather than the rigid body behaviour.It assumes that the failure occurs on a well defined slip surface and that the material behaves elastically at stress levels below failure but develops a perfectly elastic behaviour above yield.The method involves the following steps :

- 1) Determination of a yield acceleration at which a potential

sliding surface would develop a factor of safety of unity is determined.

- 2) Determination of earthquake induced acceleration in the embankment using the dynamic response analysis. 3) For a given potential sliding mass, when the induced acceleration exceeds the calculated yield acceleration, movements are assumed to occur along the direction of the failure plane and the magnitude of the displacement is evaluated by a simple double integration procedure.

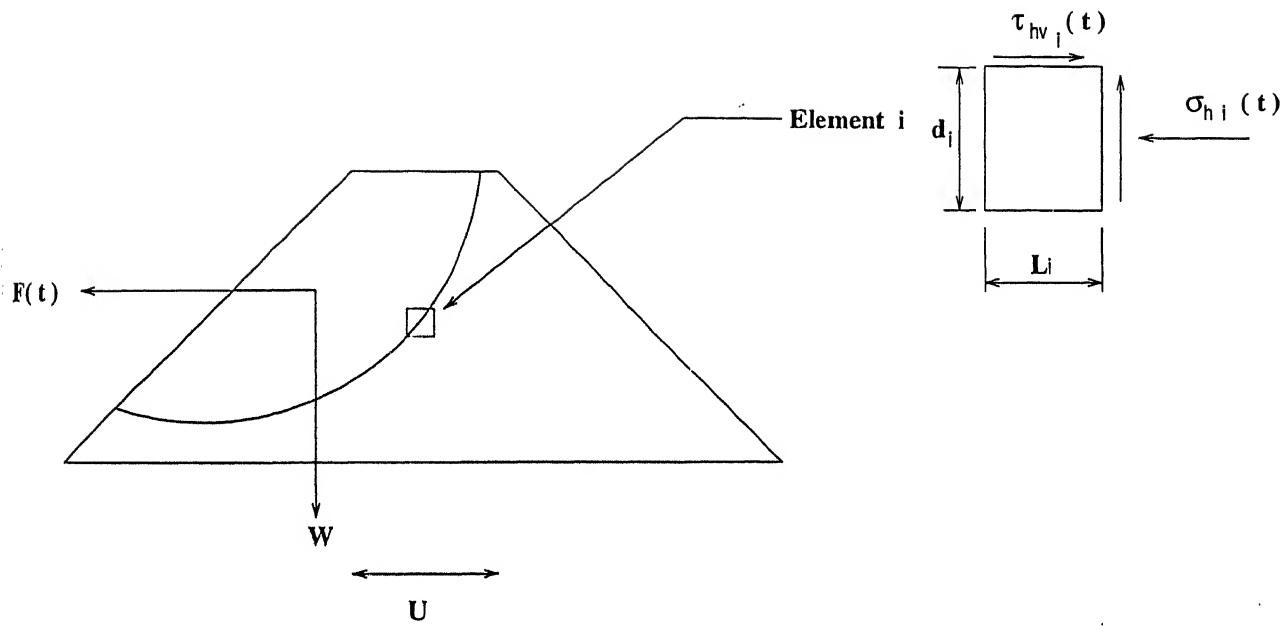
2.4.4.2 Determination of yield acceleration :

The yield acceleration (k_y) is defined as the average acceleration producing a horizontal inertia force on a potential sliding mass so as to produce a factor of safety of unity and thus cause it to experience permanent displacement. This can be achieved using one of the available methods of stability analysis. In the present study the modified Bishop method has been used to calculate the yield acceleration for a circular slip surfaces using a pseudo static analysis.

After determining the yield acceleration for a certain location of the slip surface, the next step in the analysis is to determine time history of earthquake induced average acceleration for the particular sliding mass.

2.4.4.3 Determination of earthquake induced acceleration:

In order to determine the permanent deformation for a particular slip surface, the time history of earthquake induced average acceleration must first be determined. As shown in Fig. 2.7 at each time step the forces acting along the boundary of the sliding mass are calculated from the corresponding normal and shear stress of the finite elements along that boundary. The resultant of these



$$F(t) = \sum_{i=1}^n \tau_{hv_i}(t) L_i + \sigma_{h_i}(t) d_i$$

n = number of elements along the sliding surface.

$$k_{av}(t) = F(t) / W$$

Figure 2.7 Calculation of Average Acceleration from Finite Element Response Analysis

forces divided by the weight of the sliding mass would give the average acceleration $k_{av}(t)$, acting on the sliding mass would give the average acceleration. Comparing the time history of crest acceleration with that of average acceleration for different depth of potential sliding mass, the similarity in the frequency content is readily apparent (it generally represents the first natural period of the embankment) while the amplitudes are shown to decrease as the depth of the sliding mass increases towards the base of the embankment. The maximum crest acceleration is designated by u_{max} and k_{max} is the maximum average acceleration for a potential sliding mass extending to a specific depth y . Fig. 2.8 shows a relationship showing the variation of the maximum acceleration ratio k_{max}/u_{max} with depth for a range of embankments and earthquake loading conditions. It would then be sufficient for, design purposes to estimate the maximum crest acceleration in a given embankment due to specified earthquake and use this relationship to determine the maximum average acceleration for any depth of the potential sliding mass.

Shake (Earthquake response analysis of horizontally layered site of version 1988) program has been used in this study to determine the variation of maximum acceleration with depth using some published results of response computations.

Fig 2.8 shows the results of variation of maximum average acceleration ratio with depth based on the results reported by Ambraseys and Sarma (1967) and Seed et.al. (1978 on the basis of finite element calculation). Knowing the yield acceleration and the time history of average acceleration for a potential sliding mass, the permanent displacement can be calculated using the fig. 2.9, showing the variation of y/h with k_y/k_{max} for different magnitude

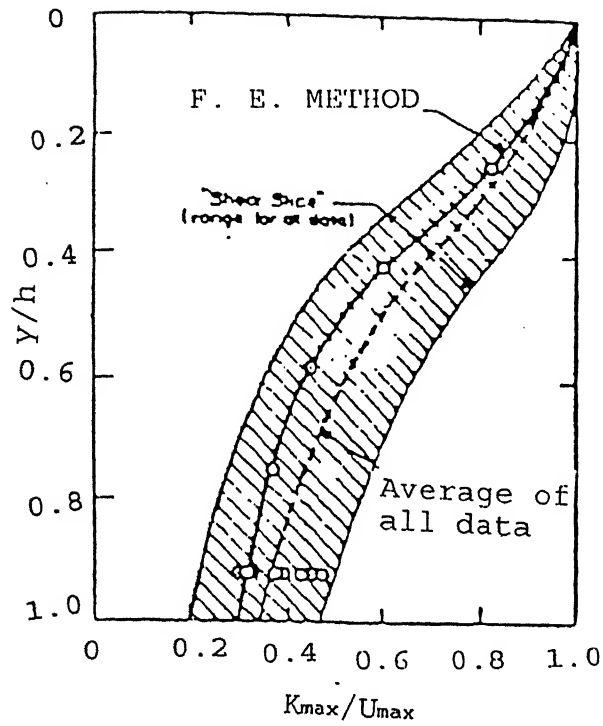


FIG. 2.8 VARIATION OF MAXIMUM ACCELERATION RATIO WITH DEPTH OF SLIDING MASS

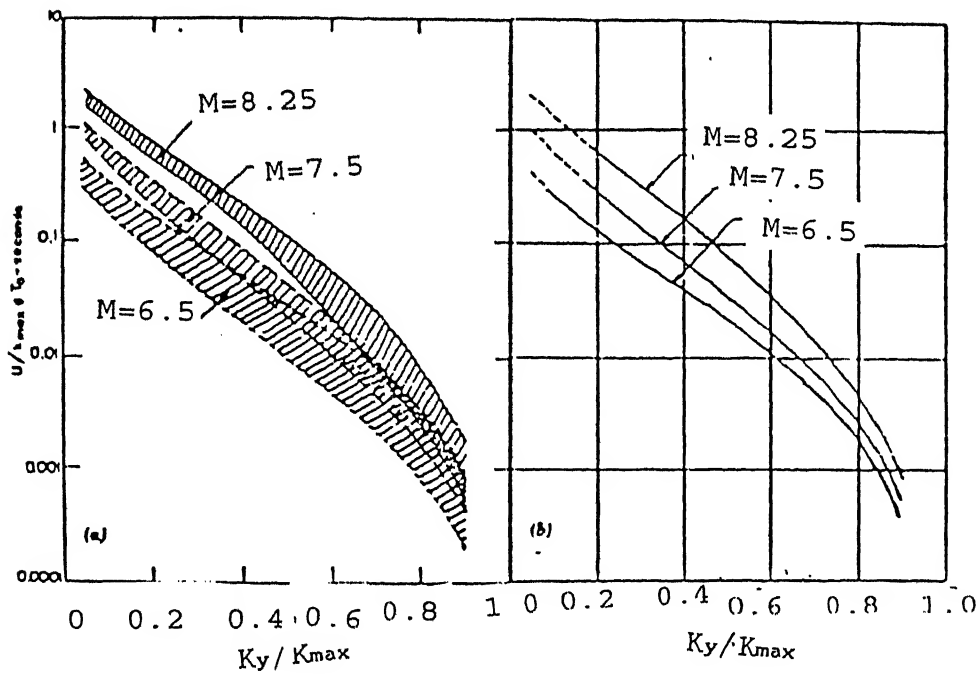


FIG. 2.9 VARIATION OF YIELD ACCELERATION WITH (A) NORMALIZED PERMANENT DISPLACEMENT (B) AVERAGE NORMALIZED DISPLACEMENT

of earthquake.

2.4.5 COMPLETE DYNAMIC ANALYSIS :

Dynamic analysis represents the state of the art for seismic analysis of uncompacted embankments subjected to strong shaking. Dynamic embankment analysis for conventional dams are described by Seed et al. (1975) Lee and Roth(1977)and Makdisi et al. (1978)Finn and Byrne (1976) Doery and Byrne(1982)describe dynamic analysis procedures applied to centreline type tailings embankments.In a dynamic analysis of a centreline embankment Lo et al.(1982)discuss the effects of assumed slimes liquefaction on stability of the embankment.

Seed(1979 b) and Finn(1982)summarize procedures by performing dynamic analyses of conventional dams respectively. In general, dynamic analyses incorporate the following steps :

- 1) Determine the preearthquake static stress in the embankment.
- 2) Determine the dynamic response of the embankment and foundation to base rock motions.
- 3) Evaluate the dynamic soil behaviour
- 4) Evaluate embankment stability .

2.4.5.1 Determine the preearthquake static stress in the embankment :

This is usually performed using a static finite element analysis to determine the initial effective normal stress and shear stress along the potential failure.These stresses are essential for proper interpretation of laboratory cyclic data.

2.4.5.2 : Determine the dynamic response of the embankment and foundation to base rock motion :

On the basis of a well instrumented earthquake in a similar geologic environment and of similar size and duration , a bed rock

acceleration time history is established. Based on this base motion time history , the response of the embankment is determined by dynamic finite element modeling ,using either equivalent linear or non linear procedures. The end result is to determine the acceleration time history at every node in the finite element mesh. These time histories must be converted to an equivalent series of uniform cyclic stress application.

2.4.5.3 : *Evaluate the dynamic soil behaviour :*

This is ordinarily accomplished by performing cyclic stress tests for conditions corresponding to those indicated by the results of static stress analysis with the laboratory results corrected to account for several factors that influence the in situ behaviour .Failure in laboratory samples may be defined in terms of initial liquefaction or with reference to a particular level of axial strain.

2.4.5.4 : *Evaluate embankment stability :*

Stability of the embankment may be addressed in terms of either stresses or strains occurring locally within the embankment. The stability of the embankment is evaluated by comparing stresses induced by the earthquake to those required to cause liquefaction or to exceed prescribed limits of local strain. The locations within the embankments for which induced stresses exceed those required to cause liquefaction or produce unacceptable strain determine the extent of liquefaction or unacceptable performance. Embankment deformations can be assessed qualitatively on the basis of strain potential for the individual elements, which corresponds to the strain to that would be experienced if the element were not constrained by surrounding soil. Elements with excessive strain potential may be considered

to offer no excessive resistance to slide movement within the embankment. Under these conditions, a stability analysis can be performed to indicate the overall factor of safety against sliding through zones of liquefaction or excessive deformation (Seed et.al. 1975). Alternatively, cyclic induced pore pressures for individual elements, together with effective stress strength parameters, can be incorporated into a limit equilibrium analysis to compute a post earthquake factor of safety. In addition, Lee and Roth (1977) recommended to calculate total embankment deformation on the basis of gravity loads and softened material properties to determine whether they lie within the acceptable limits.

2.5 Packages used :

Two software packages have been used in this investigation. they are

1. PCSTABL5
2. SHAKE

2.5.1 PCSTABL5 :

it is a personal computer based program developed by Siegel (1975) and Boutrup (1977) in FORTRAN IV language for the general solution of slope stability problems by two dimensional limit equilibrium methods. the factor of safety against instability of a slope is performed by the method of slices, modified Janbu method and Spencer method (1967) for slip surfaces of any shape.

The PCSTABL5 features a random search for generation of potential failure surfaces for subsequent determination of more critical surface and their factor of safety. One technique generates circular surfaces, another surfaces of sliding character and third more general irregular surfaces of random

shape. This program also handles the heterogeneous soil system, anisotropy soil strength properties, excessive pore pressure due to shear, static ground water and surface water ,pseudo static earthquake loading and surcharge boundary loading.

2.5.2 SHAKE :

Shake, a personal computer based program is developed by Seed H. B. Schnabel B. and Lysmer J.(1972) which is later modified by Sun J.and Lai S. It computes the responses in a system of homogeneous, viscoelastic layers of infinite horizontal extent subjected to vertically travelling shear waves. The program is based on the continuous solution to the wave equation (Kanai 1951)adapted for use with transient motions through the Fast Fourier Transform algorithm (Cooley and Tukey, 19650. The non linearity of the shear modulus and damping is accounted for by the use of equivalent linear soil properties (Idiris and Seed 1968 Seed and Idris 1970) using an iterative procedure to obtain values for modulus and damping compatible with the effective strain in each layer. The following assumptions are made in this analysis :

- 1) Soil system is infinitely extended in the horizontal direction
- 2) Each layer is completely defined by its value of shear modulus, critical damping ratio density and thickness .
- 3) The response in the system are caused by the upward propagation of shear waves from the underlying rock formation.
- 4) The shear waves are given as acceleration values of equally spaced time intervals. Cyclic repetition of the acceleration time history is implied in the solution.
- 5) The strain dependence of the modulus and damping is accounted for by an equivalent linear procedure based on an average effective strain level computed for each layer.

The program is able to handle systems with variation in both moduli and damping and takes into account the effect of the elastic base. The motion used as a basis for the analysis, the object motion, can be given in any one layer in the system and new motions can be computed in any other layer.

layered site using different earthquake record data such as Pasadena earthquake(1952), Kerntaft earthquake etc. program has been used in this study to determine the variation of maximum acceleration with depth using some published results of response computations. Following sets of operation can be performed by this program :

- 1) By reading the input motion it determines the maximum acceleration, scales the values and computes the predominant period.
- 2) By reading the soil deposit properties, it computes the fundamental period of the deposit. It computes the maximum stress and strains in the middle of each sub layer and modifies the value of modulus and damping with a specified percentage of maximum strain.
- 3) It computes the new motion at the top of any sublayer inside the system or outcropping from the system which can be printed, plotted or punched as per the requirement..
- 3) It also computes the response spectra for the motion.
- 4) Amplification function between any two sublayers can be computed, printed and plotted.
- 5) Without changing the predominant period or duration of the record time interval can be increased or decreased.
- 6) Computed motion can be set as a new motion.
- 7) Stress or strain time history in the middle of any sublayer can

be computed, printed and plotted.

These operation can be performed by exercising the various available options in the program.

CHAPTER 3

EXPERIMENTAL DETAILS

3.1 General :

This chapter includes the source of material, details of their properties , preparation of the sample, type of test performed, test details and test results..

3.2 Source of Material :

Three types of flyash samples, obtained from three different sites, have been investigated in this program. Samples were obtained from Satpura Thermal Power Plant(STPP) Sarni dist. Betul, M.P., Korba Super Thermal power Plant(KSTPP) Korba dist. Bilaspur; M.P. and Hansdeo Thermal Power Plant(HDTPP) Korba west dist. Bilaspur M.P.. All the samples were obtained from ash disposal ponds of those sites.

3.3 Properties Of Fly ash :

The physical and chemical behaviour of fly ash is governed by several factors such as coal source, degree of coal pulverization, design of boiler unit, loading and firing conditions and handling and storage methods. A change in any of the above factors can result in detectable changes in the ash produced and it's properties

Thus it is not surprising that a high degree of variability can occur in ash properties not only between power plants but within a single power plant. The degree to which any change affects the utilization potential of ash is a function of nature and degree of changes, and the particular application for which the ash might be utilized. In this investigation following

distribution, specific gravity, optimum moisture content, maximum dry density, shear strength parameters, and steady state strength.

Grain size distribution curve:

Fig.3.1 represents the combined results of the sieve analysis and hygrometer analysis. The grain size distribution analysis gives an idea about type of material and gradation. It is clear from the Fig.3.1 that the samples used are silt to sand sized particles.

Specific gravity:-

Specific gravity tests were done in the laboratory with the help of specific gravity bottle. Specific gravity of KSTPP fly ash reported by Wasan (1995) has been used here. The results are given in the Table 3.1.

Standard Procter Test:-

Standard Procter test was carried out to determine the maximum dry density and optimum moisture content of STPP and HDTPP ash samples. Standard Procter test result of KSTPP sample given by Wasan (1995) has been used here. these results are given in Table 3.1.

Shear strength Parameter:-

For saturated ash samples, effective strength parameters were determined by consolidated undrained triaxial test with pore pressure ($\bar{C}\bar{U}$) measurement. STPP samples have been tested at 90% and 95% maximum dry density, whereas HDTPP sample has been tested at 95% maximum dry density. For KSTPP the shear strength parameter given by Wasan (1995) is used in the investigation. The shear

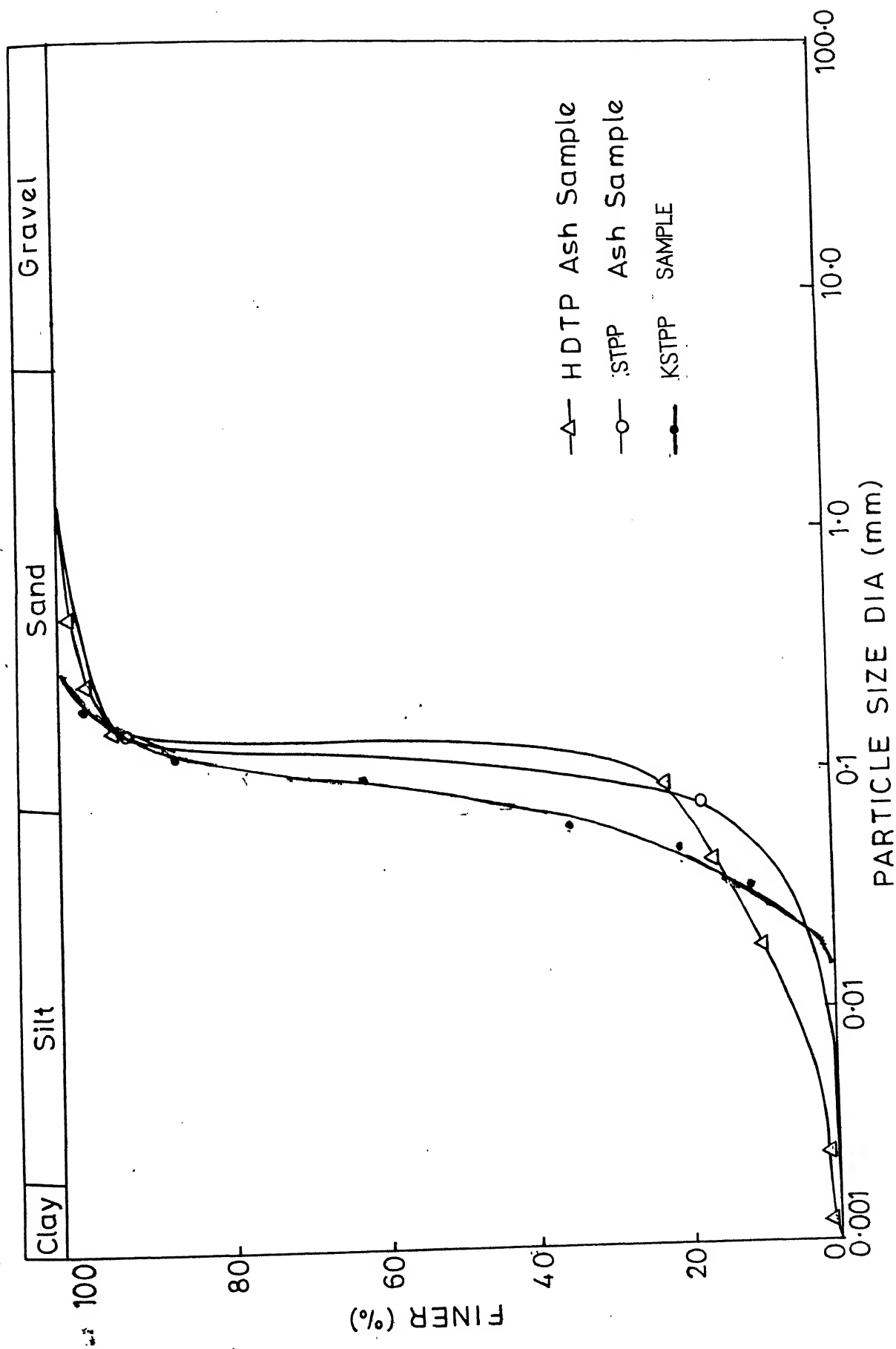


Fig.3.1 Gradation Curve for Ash Samples

at 95% maximum dry density. For KSTPP the shear strength parametre given by Wasan M.(1995) is used in the investigation. The shear strength parametres (cohesion (c') and effective friction angle (ϕ')) for all the three sites are summerized in the Table 3.1.

Table 3.1 Geotechnical properties of samples

Sample 1. STPP Fly ash

Specific Gravity	1.98
Optimum Moisture Content	33%
Maximum Dry Density	1.11 gm/cc
Shear strength Parametre	
C' }	0
ϕ' } (95% M.D.D.)	35.5°
C' }	0
ϕ' } (90% M.D.D.)	33.7°

Sample 2. HDTTP Fly Ash

Specific Gravity	1.94
Optimum Moisture Content	32%
Maximum Dry Density	1.145 gm/cc
Shear strength Parametre	
C' }	0
ϕ' } (95% M.D.D.)	31.5°

Sample 3. KSTPP Fly ash

Specific Gravity	1.76
Optimum Moisture Content	41%
Maximum Dry Density	.98 gm/cc
Shear Strength Parameter	
C' }	0
ϕ' } 95% (MDD)	30.0°

3.4 Sus Test :

In order to determine the steady state strength of various ash consolidated undrained triaxial test with pore pressure measurement has been carried out on samples of 38.1 mm. diameter and 76.2 mm. high sample. The back pressure equal to cell pressure of 1.5 Kg/cm² is used to saturate the sample. To ensure the complete saturation Bishop's parametre ($B = \frac{\Delta u}{\Delta \sigma_3}$) was checked and B nearly equal to unity ensured practical limit of 100% saturation. After saturation, the sample has been consolidated for eight hours at cell pressure equal to 2.5 Kg/cm² and back pressure of 1.5 Kg/cm² i. e. effective consolidation pressure of 1 kg/cm² and then the sample was sheared using constant rate of shear strain of 6 mm/min.. In case of non cohesive soil such fly ash is no pore pressure lag is likely to occur at the applied strain rate of 6mm/min.. The deviatoric stress is calculated after applying the area correction from the proving ring reading and the strain in the sample is measured from a dial gauge. It has been observed that the ash sample attains its steady state generally at 15-16 % strain. At steady state the shear stress, deviator stress and effective minor principal stress become more or less constant with further the increase of strain. Graphs were plotted between effective principal stress versus strain and deviator stress versus strain and value of q_s and $\bar{\sigma}_{3s}$ were taken from these graphs to calculate the S_{us} .

3.4.1 Test Sample :

Three types of samples have been prepared for consolidated undrained test with pore pressure measurement. They are as follows:-

- 1) Compacted sample
- 2) Tube sample

3) Loose sample

Compacted sample:

Based on standard Procter test results, samples were prepared at 85%, 90%, 95% and 100 % Standard Procter dry density in miniature Procter compaction sampler. Fly ash of required weight has been taken in china bowl and mixed thoroughly with required quantity of water. Then it is compacted in miniature Procter sampler in three layers and each layer was compacted twenty five times. For STPP no test has been carried out at 100% maximum dry density because it has been observed that samples tested is dilating at 90% and 95% of Standard Procter dry density shows a dilating tendency and therefore it was decided to not to test it as it will not likely to liquefy.

Tube sample:

Fly ash was thoroughly mixed with tap water (1:10) to make it in slurry form and then laboratory consolidated fly ash samples were prepared by sedimentation. The slurry was poured in a tube fitted with porous stone covered with filter paper at top and bottom and allowed to consolidate under its own weight. The excess water is allowed to escape taken out through the bottom porous stone and after that a porous stone fitted with filter paper at top and bottom is placed over the sample and a desired load is placed over it through a hanger arrangement Sample is then allowed to consolidate for next few days. Samples so formed was transferred into the miniature compaction sampler carefully to allow minimum disturbance and was cut in standard length by means of sharp edge. The STPP samples were consolidated in the tube at 0.3 kg/cm^2 , 0.6 kg/cm^2 and 0.9 kg/cm^2 pressure and HDTTP samples

were prepared at consolidation pressure of 0.6 kg/cm^2 , 0.9 kg/cm^2 , and 1.2 kg/cm^2 .

Loose sample:

Undisturbed samples taken from field generally get disturbed during sampling transporting and testing. Also it is very difficult to prepare compacted sample at less than 85% MDD or at low consolidation pressure. In order to get good quality of loose sample for testing, it was decided to prepare loose sample in the cell itself. using vacuum technique.

3.5 Test Results :

Sust ests were performed on the Procter compacted samples, tube consolidated samples and the loose sample. Fig.3.2, Fig.3.3 and Fig.3.4 show the variation of deviator stress versus strain of compacted samples of STPP, HDTPP and KSTPP samples, respectively. From these figures it is clear that deviator stress increases with dry density of sample. The deviator stress also increases with the strain and eventually it becomes constant at a very high strain.

Fig.3.5 to Fig. 3.7 shows the variation of change in pore pressure with strain for compacted samples of STPP, KSTPP and HDTPP, respectively. It is clear from those results that the variation in pore pressure with strain is much higher in loose samples than in dense samples and the variation of pore pressure gradually decreases as the density increases. Also at higher strain, change in pore pressure becomes more or less constant. In case of STPP sample change in pore pressure for 90% and 95% sample (Fig.3.5) is found to be negative at higher strain i.e. samples are dilating at those densities.

Fig.3.8 to Fig. 3.10 show the variation of effective minor principle stress versus strain for the compacted samples of STPP,

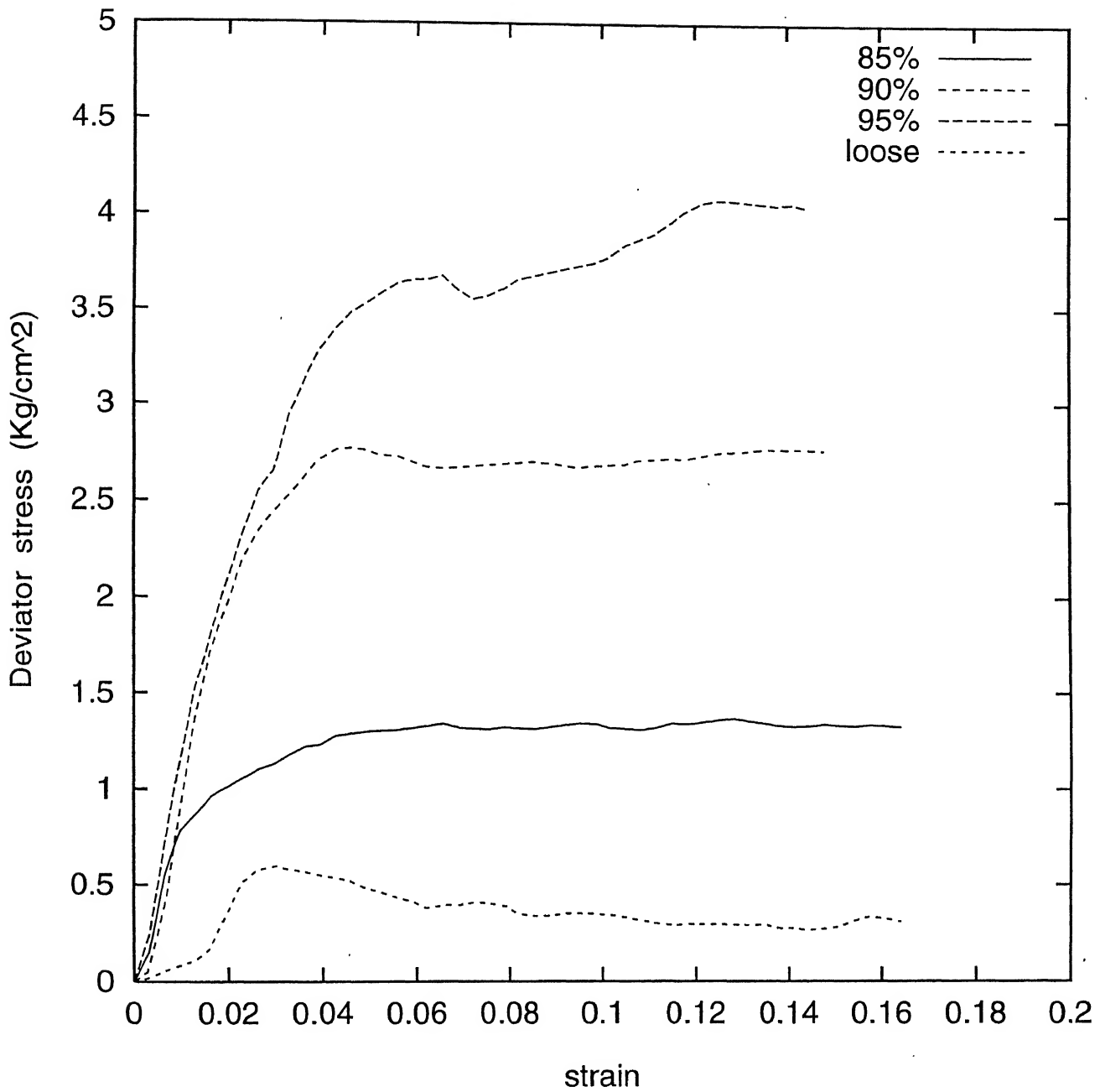


Fig. 3.2 variation of Deviator stress with strain (STPP)

CONVERSION FACTOR - $1 \text{ Kg/cm}^2 = 100 \text{ kN/m}^2$

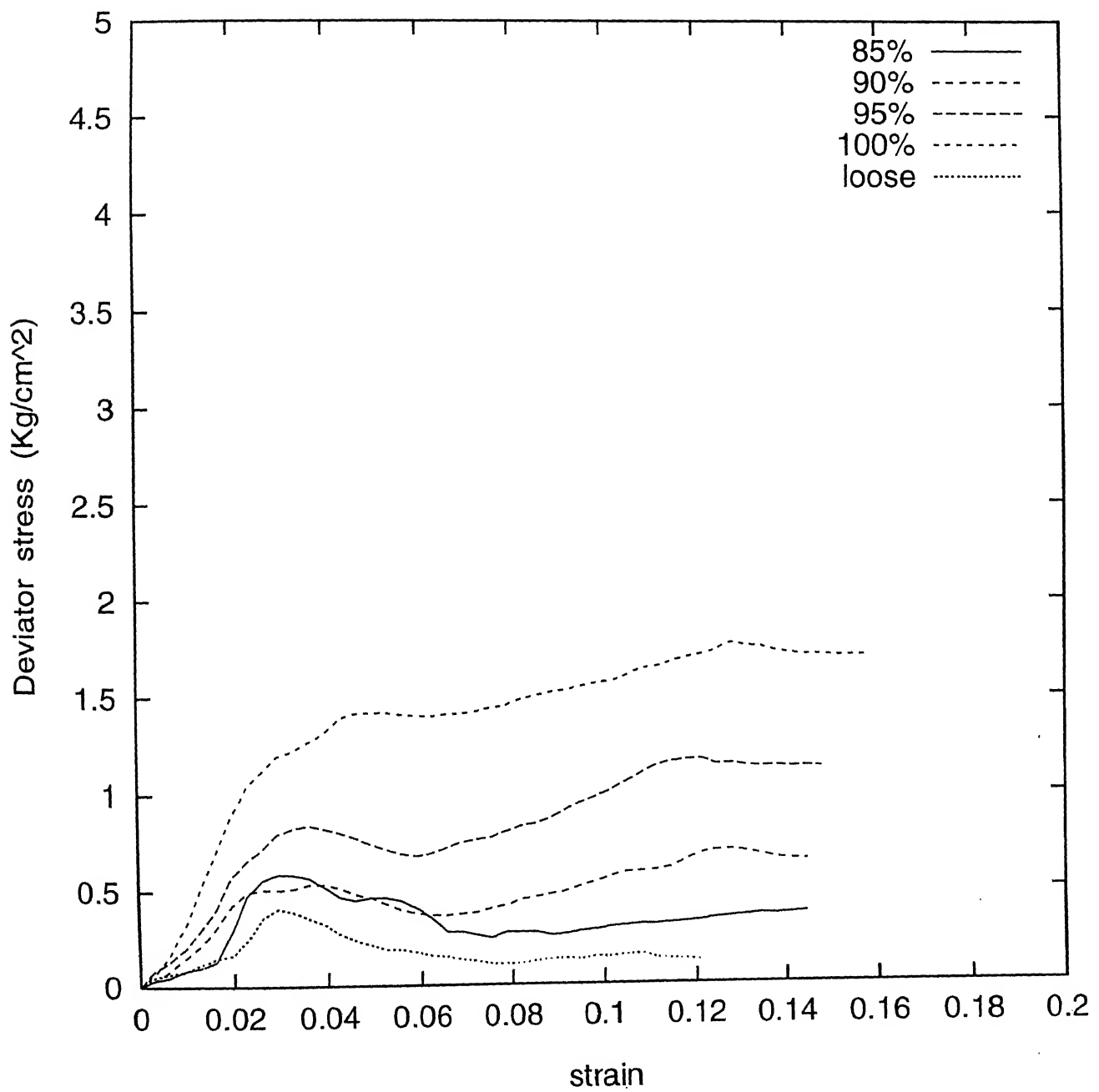


Fig. 3.3 variation of Deviator stress with strain (HDTTPP)

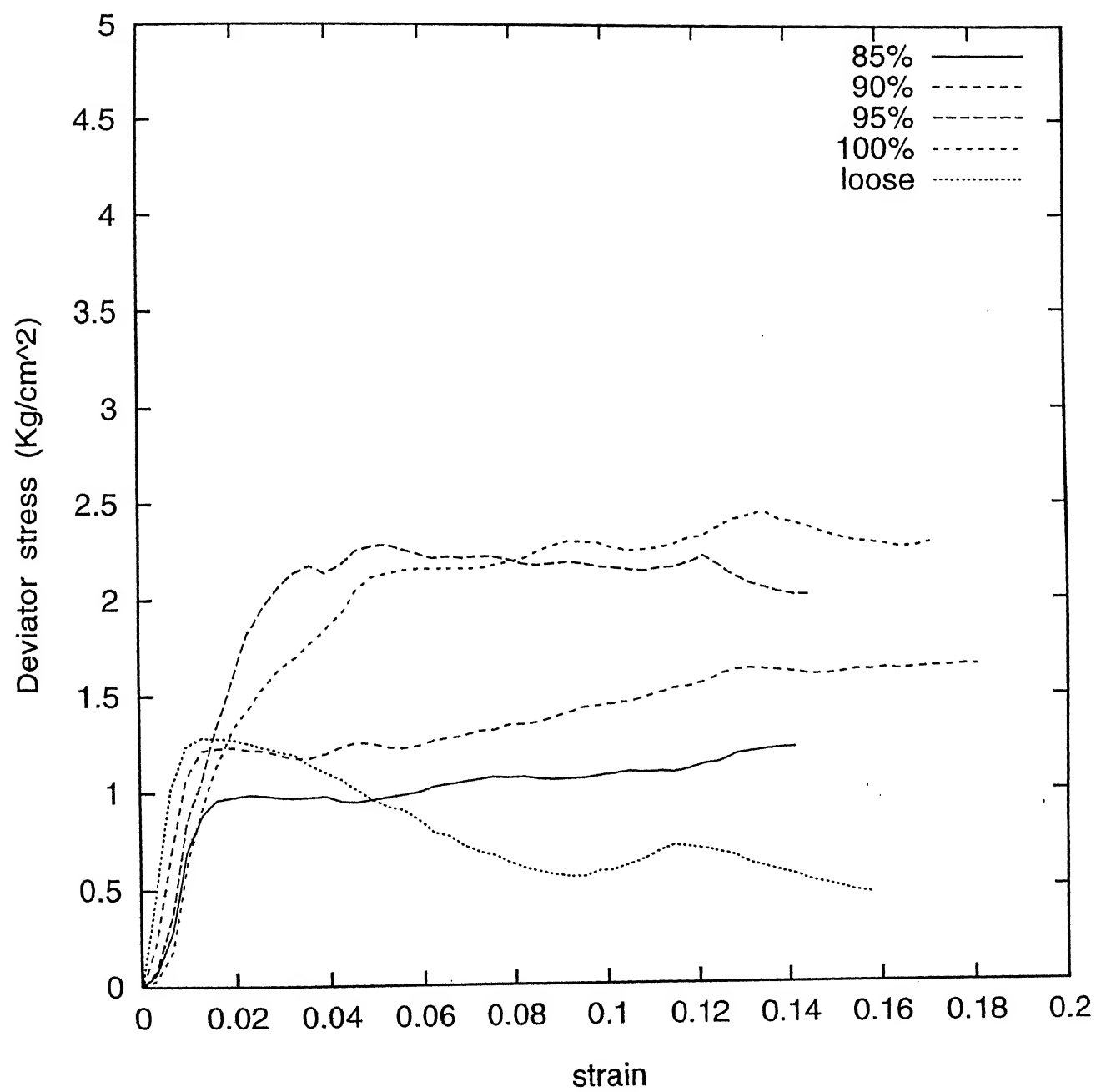


Fig. 3.4 Variation of Deviator stress with strain (KSTPP)

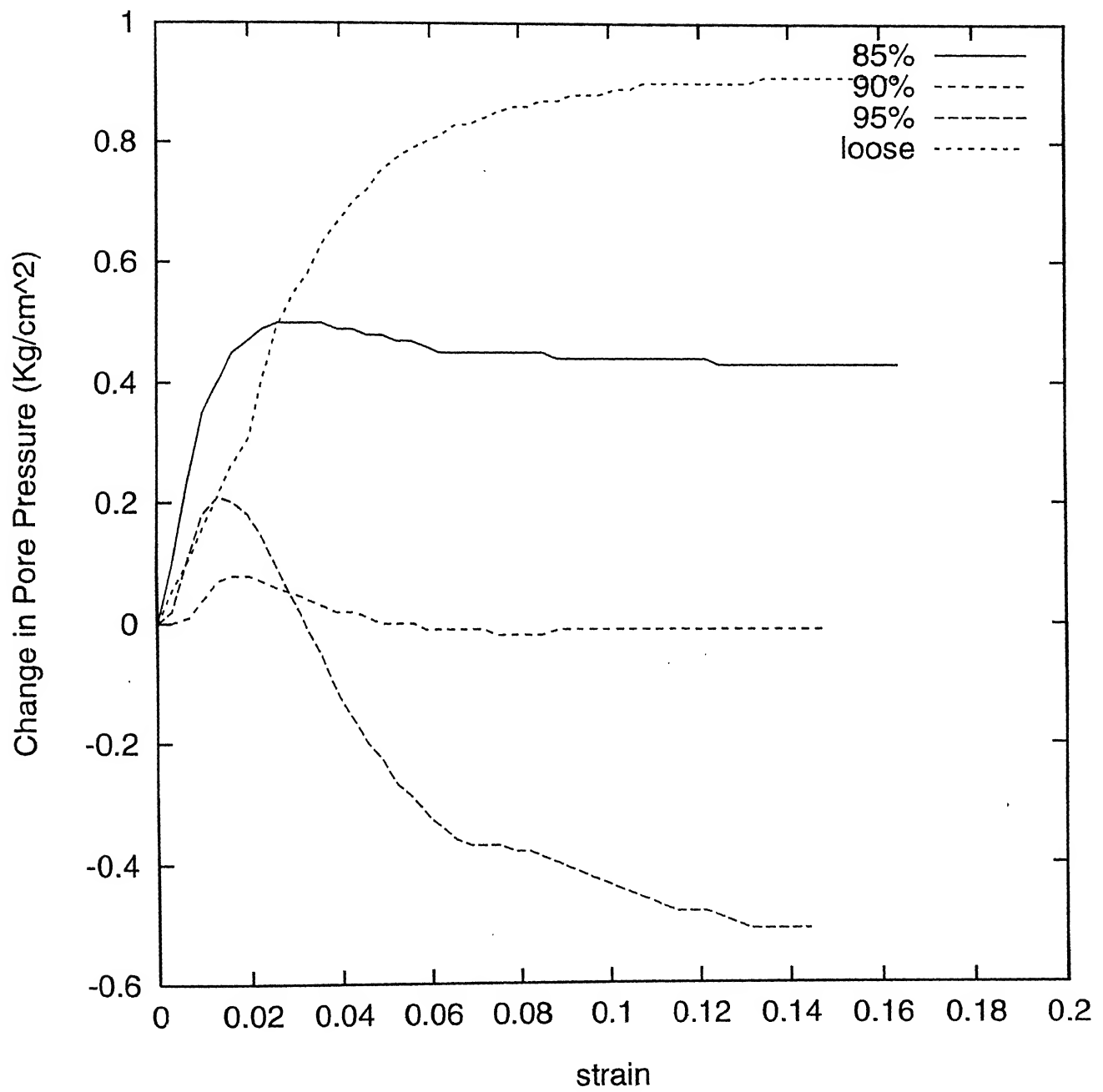


Fig. 3.5 variation of EMPS with strain (STPP)

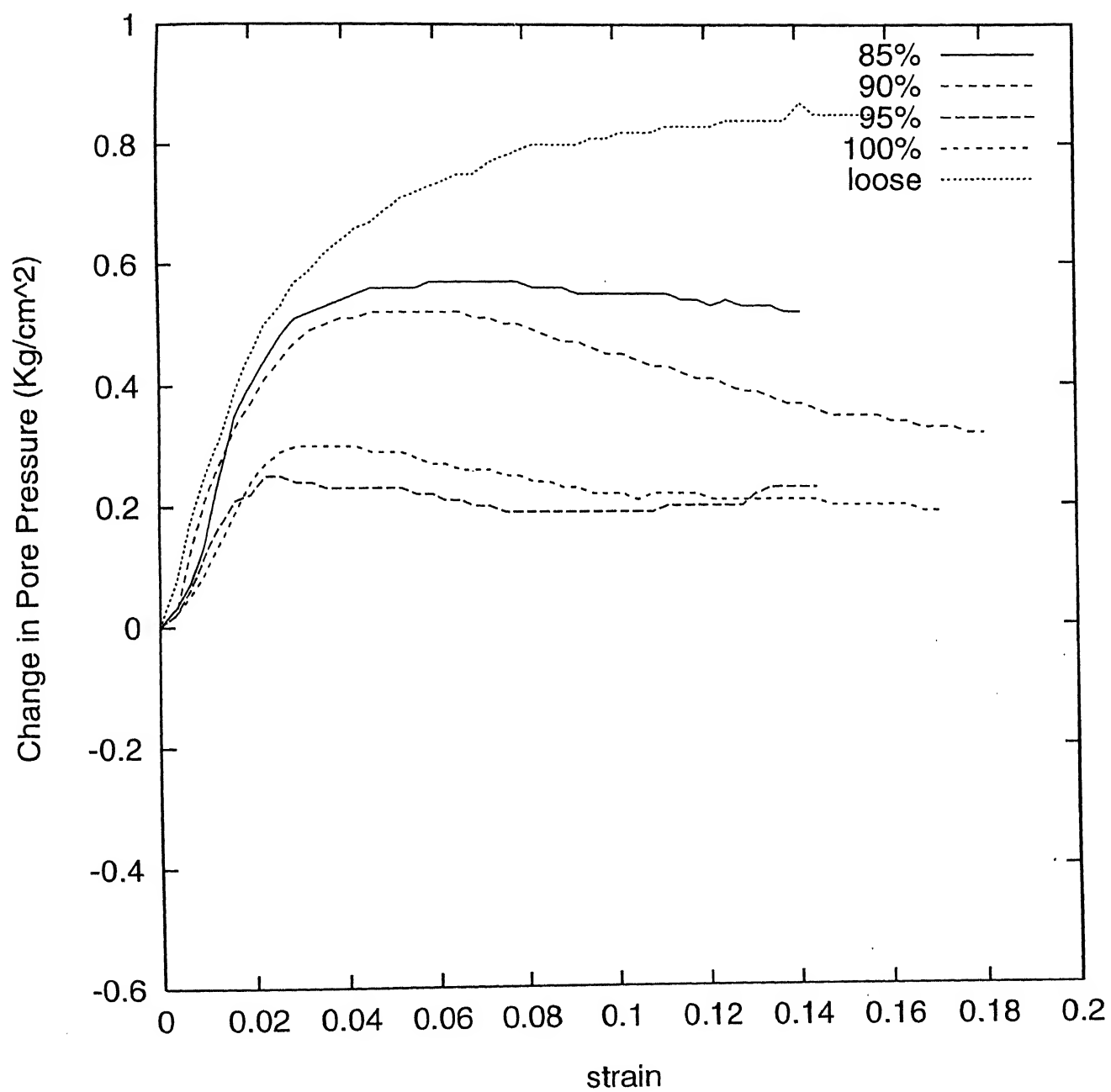


Fig. 3.6 variation of Pore Pressure with strain (KSTPP)

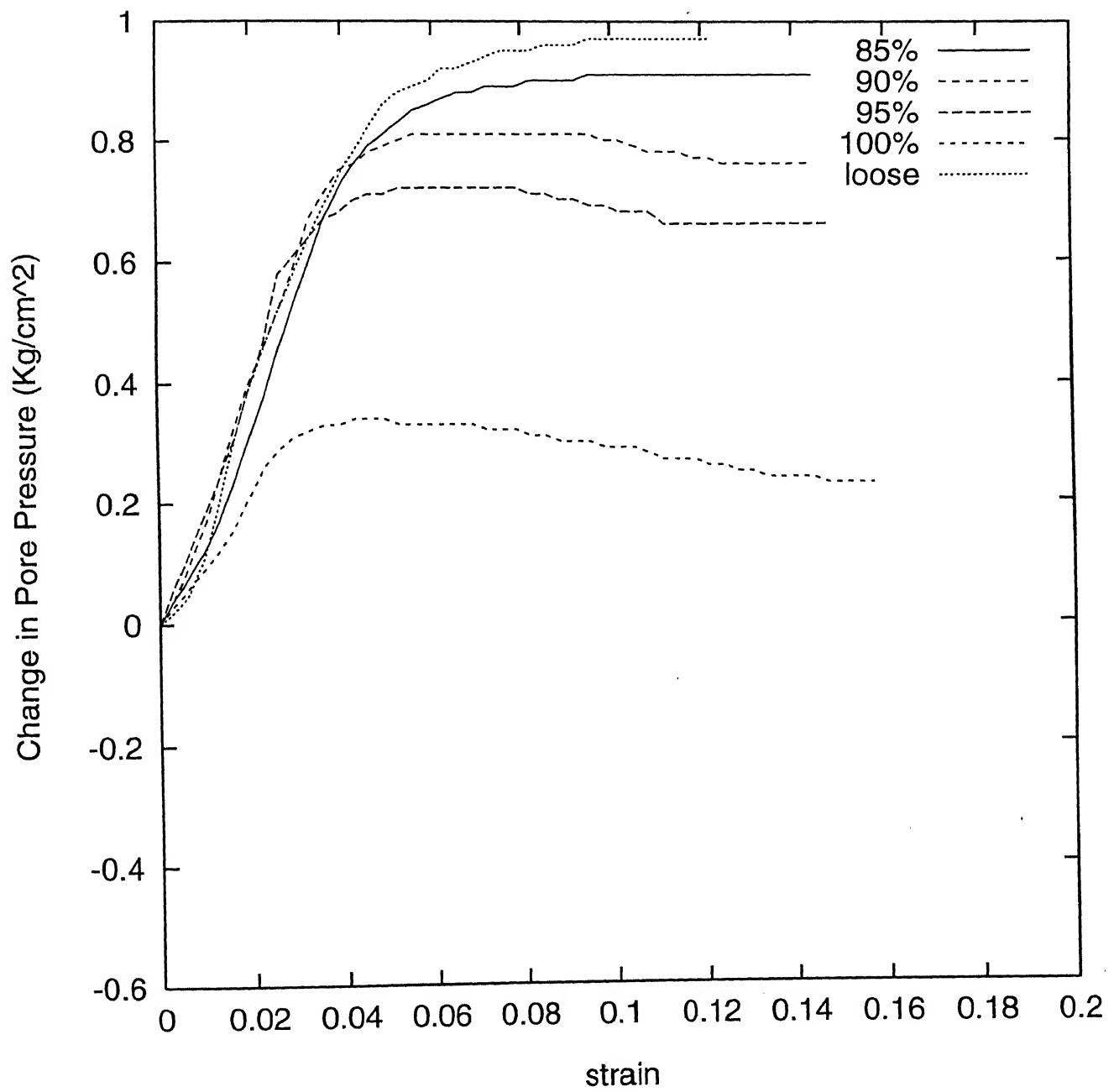


Fig. 3.7 variation of pore pressure with strain (HDTPP)

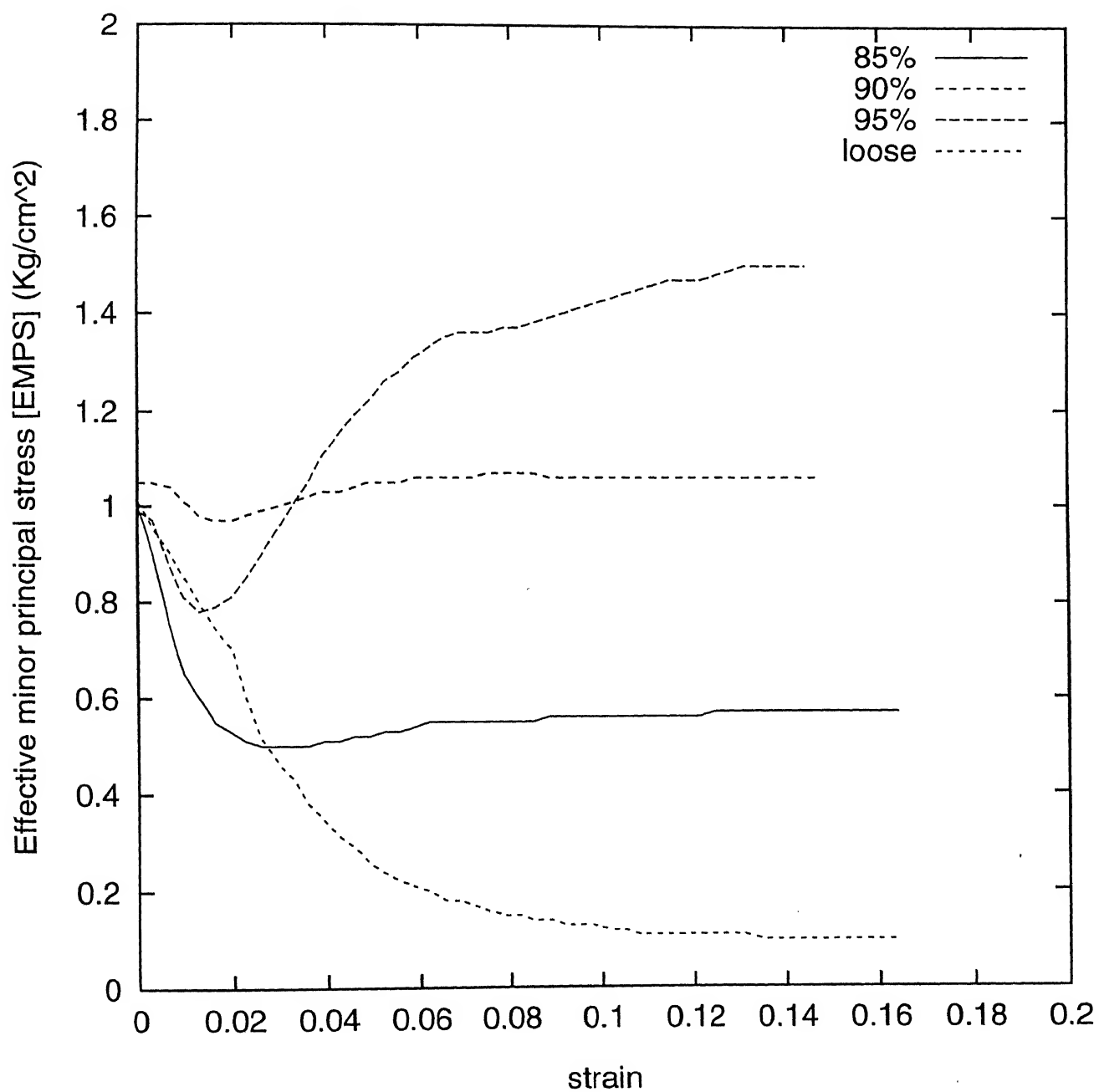
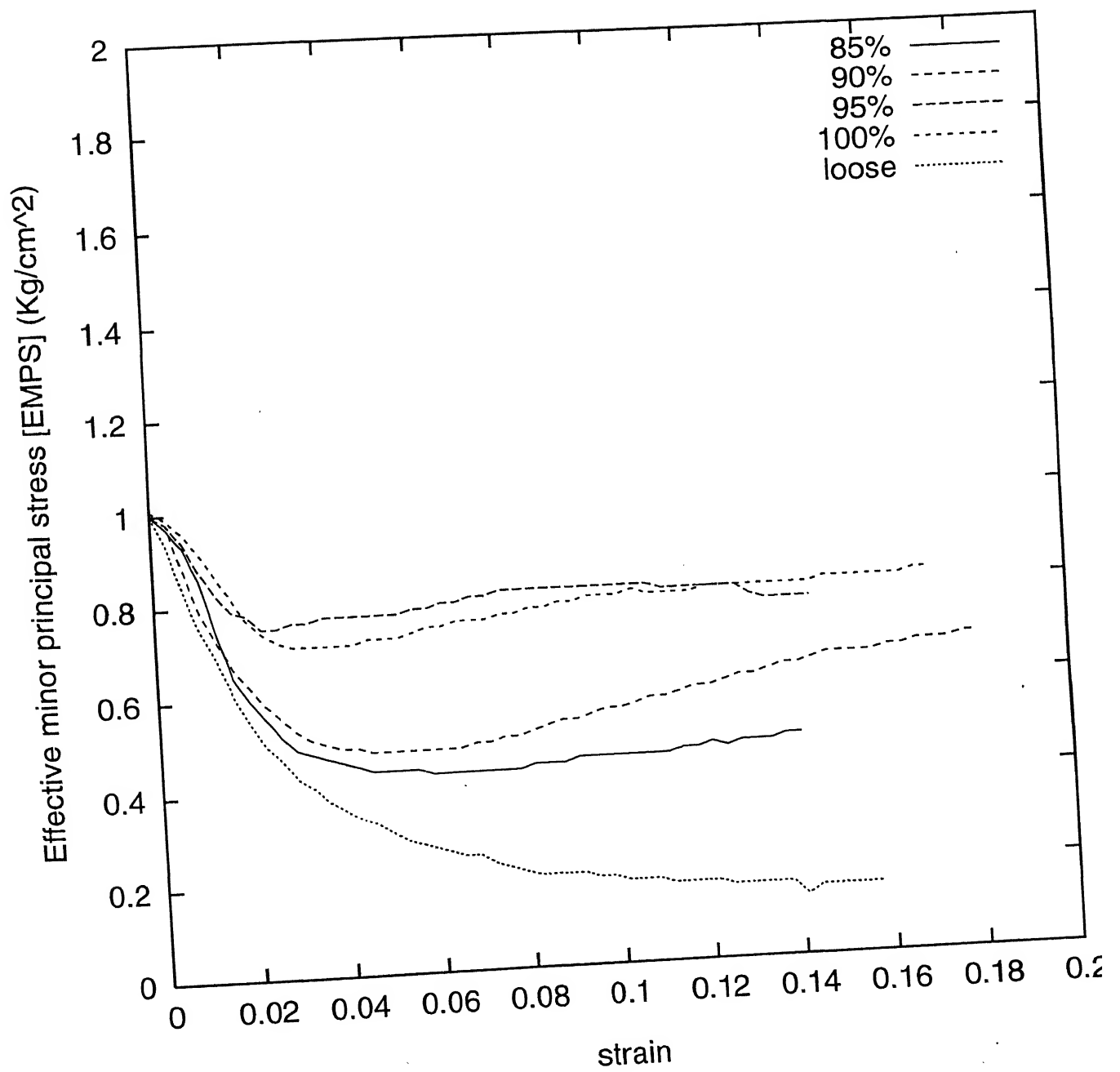


Fig. 3.8 Variation of [EMPS] with strain (STPP)



variation of [EMPS] with strain (KSTPP)

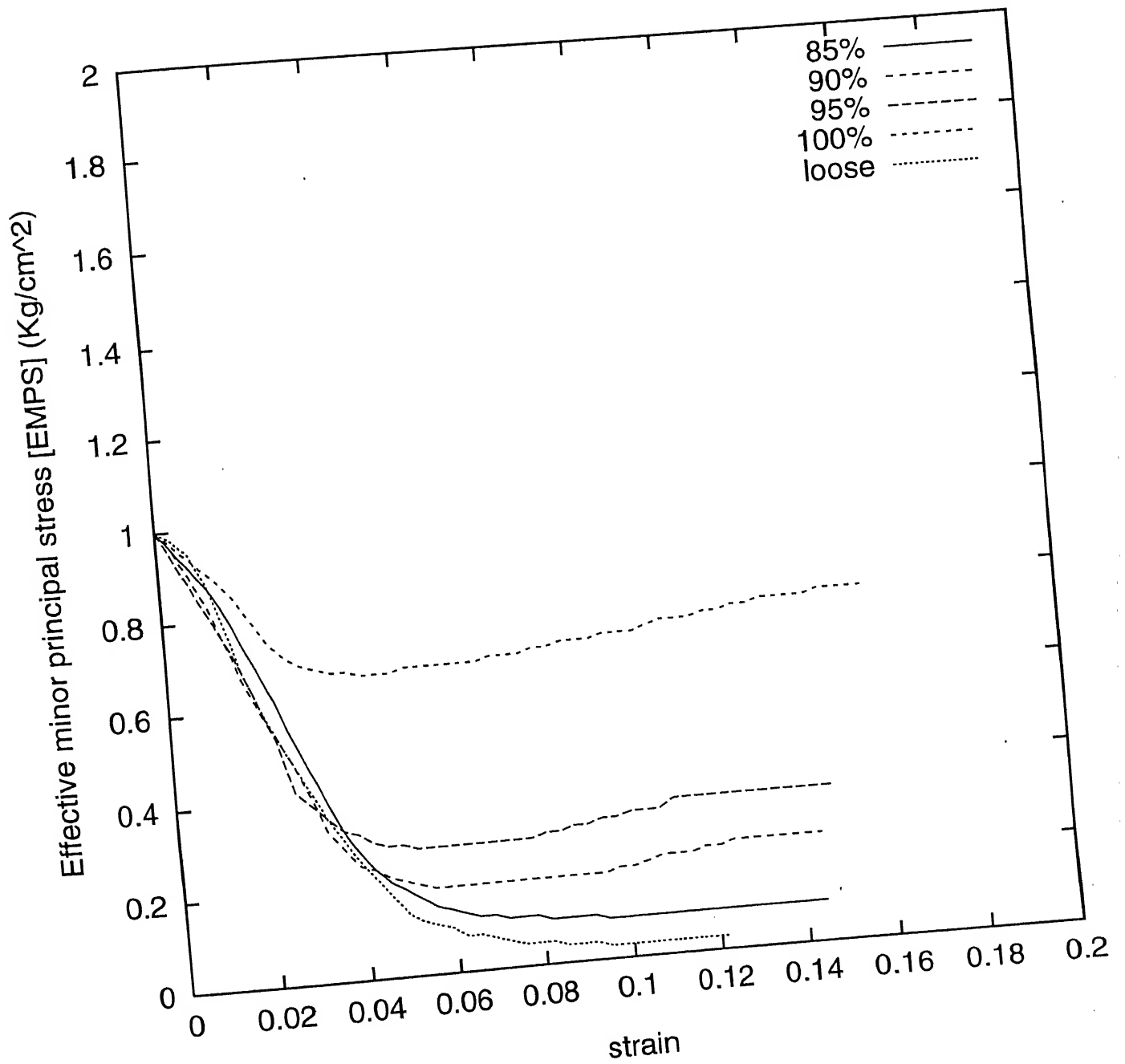


Fig 3.10 Variation of [EMPS] with strain (HDTTP)

KSTPP and HDTTP samples. These results are mirror image of the pore pressure variation versus strain, ofcourse the magnitude is different.

Fig. 3.11 and Fig.3.12 show the variation of deviatoric stress versus strain of STPP and HDTTP tube samples respectively. It is clear from these figures that the deviator stress increases with increaes of consolidation pressure. Fig. 3.13 and Fig.3.14 show the variation of change in pore pressure with strain of STPP and HDTTP samples respectively. Fig.3.15 and Fig.3.16 show the variation of effective minor principal stress versus strain of STPP and HDTTP tube samples. These test resultsa figure indicate that the behaviour of tube samples is dilative in nature. Low confining pressure during the test is probably one of the reasons for the dilative nature of the sample.

Steady state shear strength has been calculated from the ($\bar{C}\bar{U}$) test results.

SSL For Ash sample :

The S_{us} values for all the test results are calculated from the equation 2.2 taking the difference of principal stress, effective minor principal stress and change of pore pressure at steady state. Figs. 3.2 to Fig. 3.4 gives the difference of principal stress at steady state for compacted and loose samples and figs. 3.11 to Fig.3.12 for tube samples. The change in pore pressure is taken from Fig. 3.5 to Fig. 3.7 for STPP KSTPP and HDTTPsample, respectively and effective minor principal stress at steady state is taken from Fig.3.8 to Fig 3.10for compacted and loose ash samples. Similarly for tube samples the respective values were taken from Figs.3.13 to 3.16. In Table 3.2 S_{us} value and corresponding void ratio of compacted samples and loose samples are summerized. S_{us} value of tube samples are summerized

CENTRAL
I.I.T., K.
Lab. No. A.121510

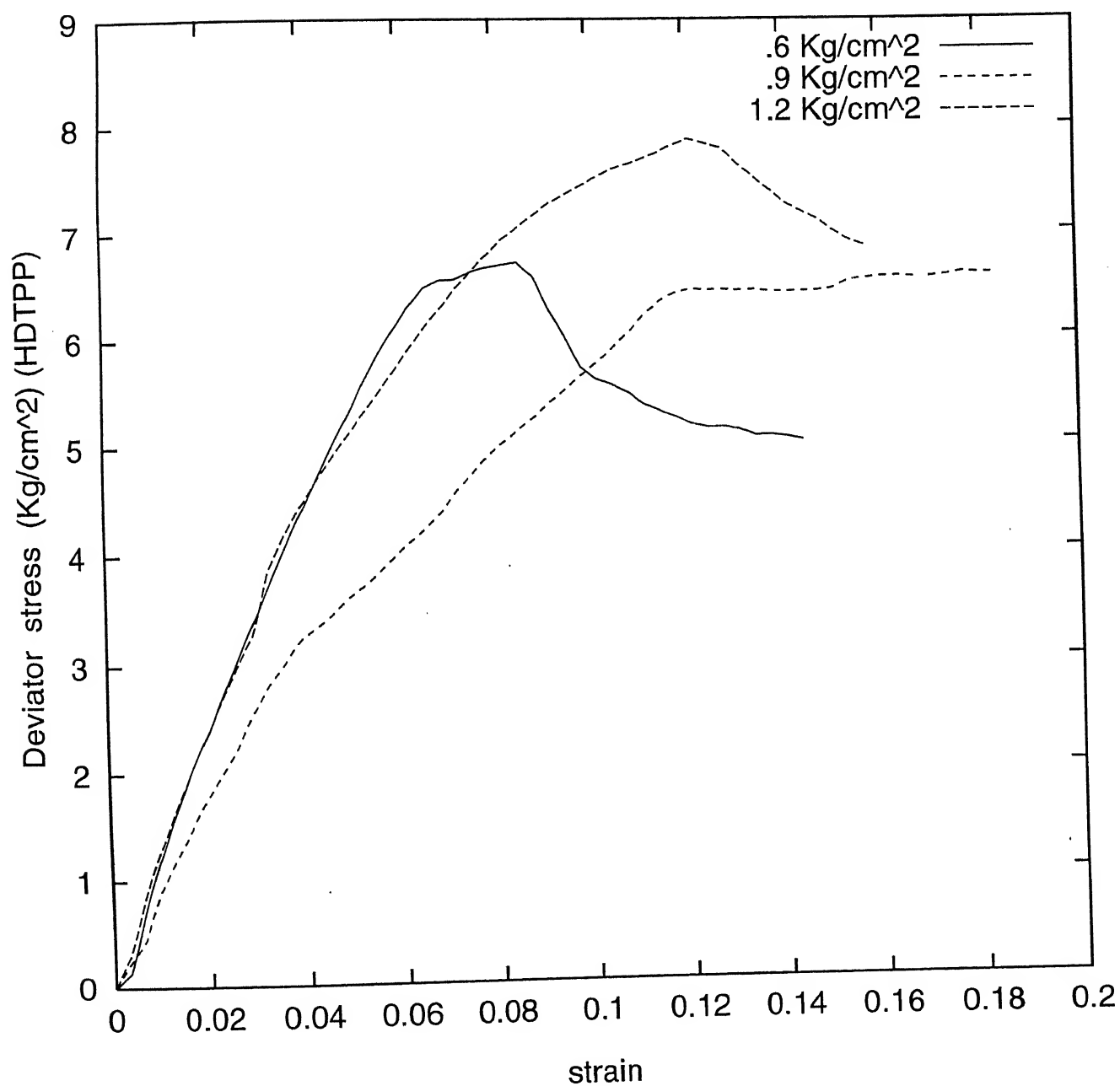


Fig. 3.11 Variation of Deviator Stress vs. Strain (HDTTPP)

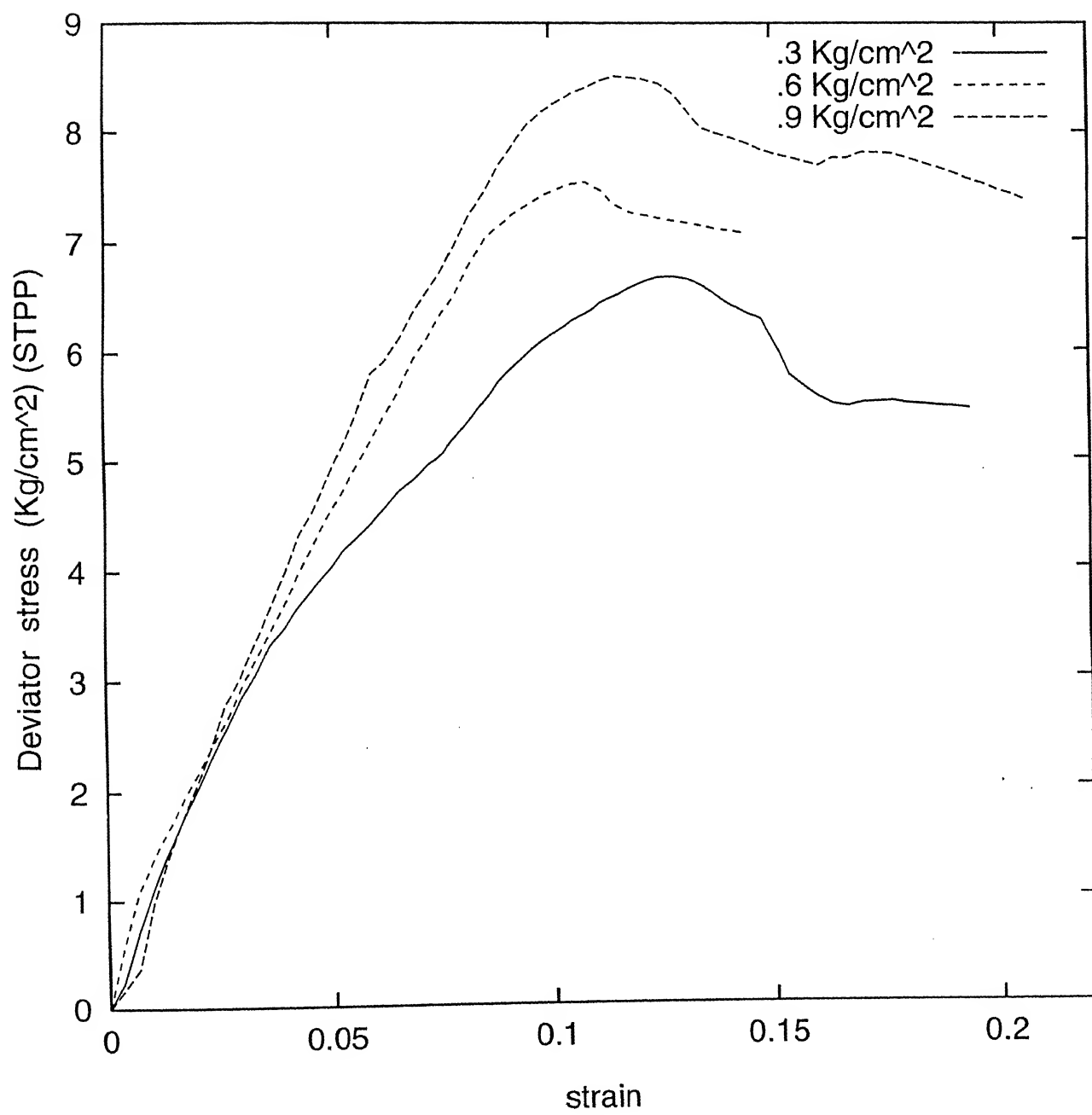


Fig. 12 Variation of deviator Stress vs. Strain(STPP)

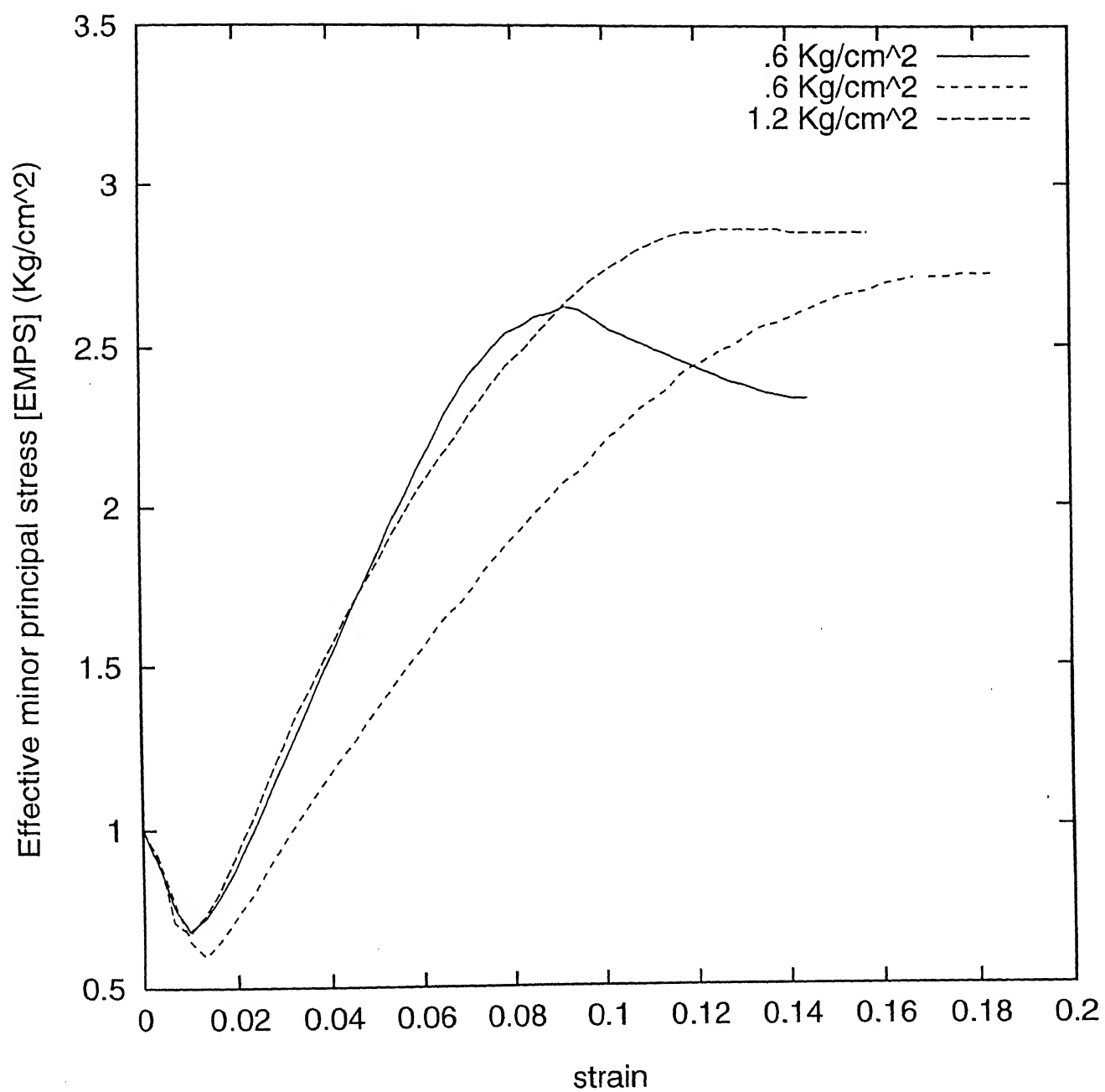


Fig. 3.13 Variation of [EMPS] with strain (HDTTP)

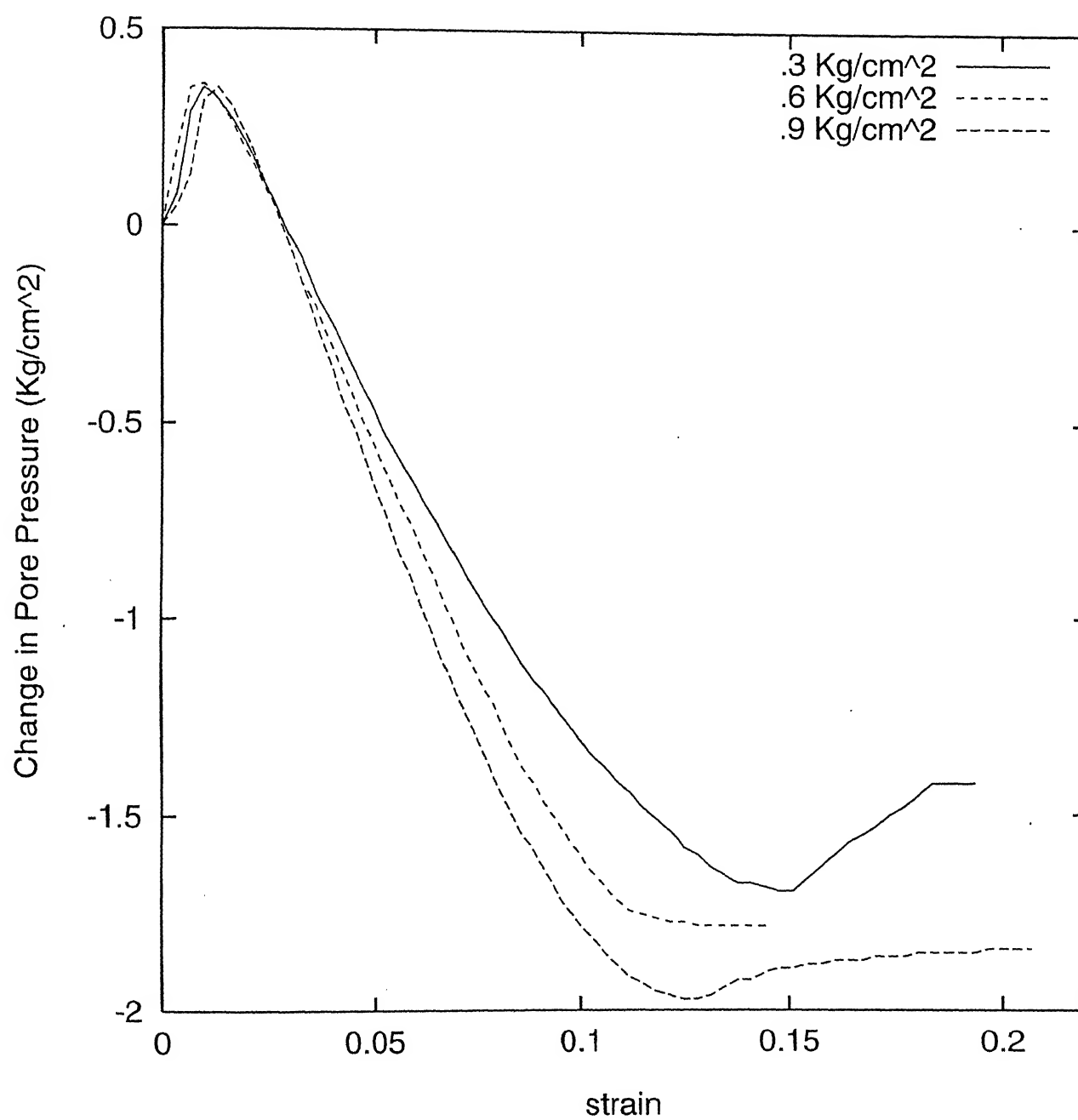


Fig. 3.14 Variation of Pore Pressure with strain (STPP)

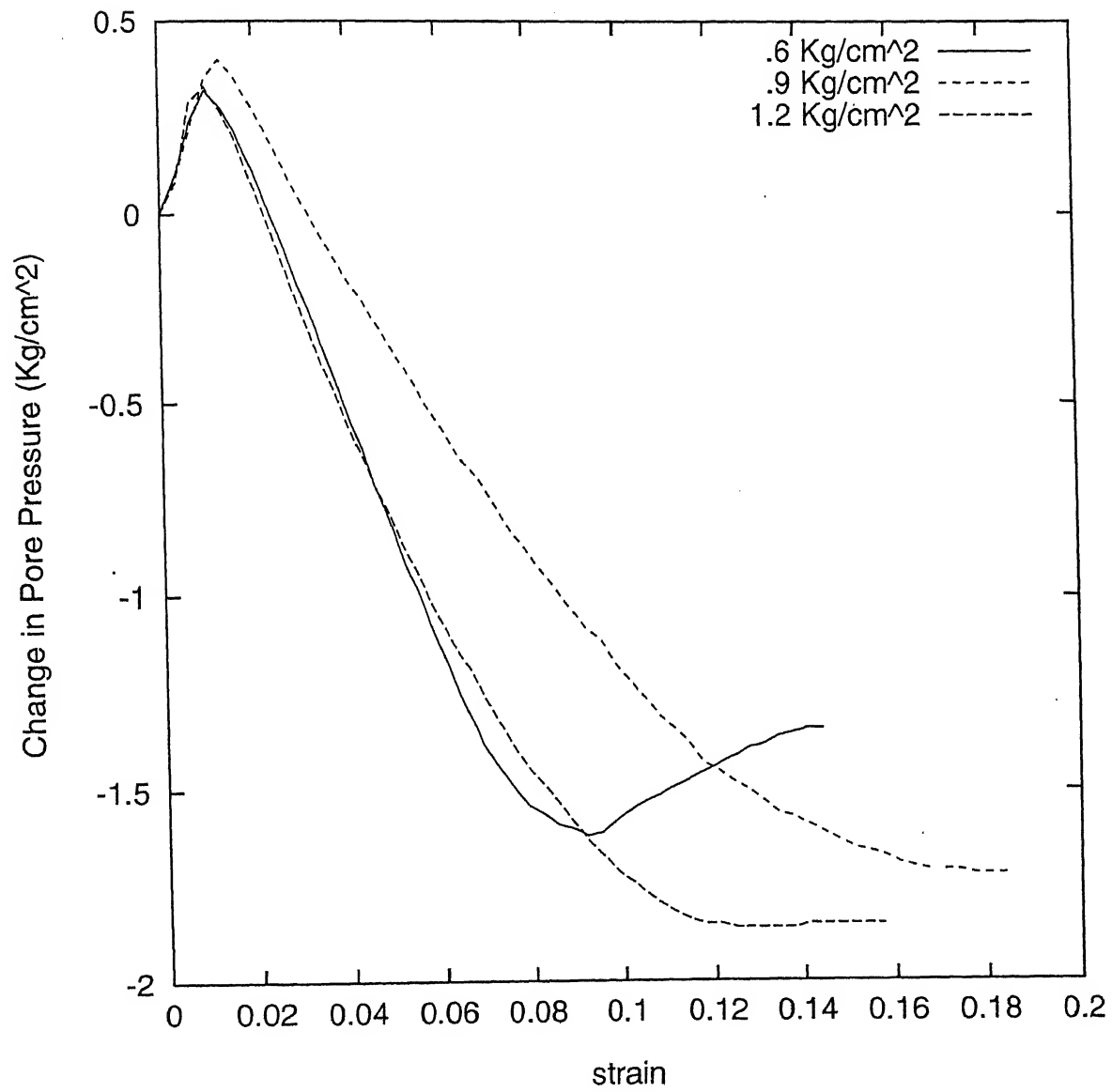


Fig.3.15 Variation of Pore Pressure with strain (HDTPP)

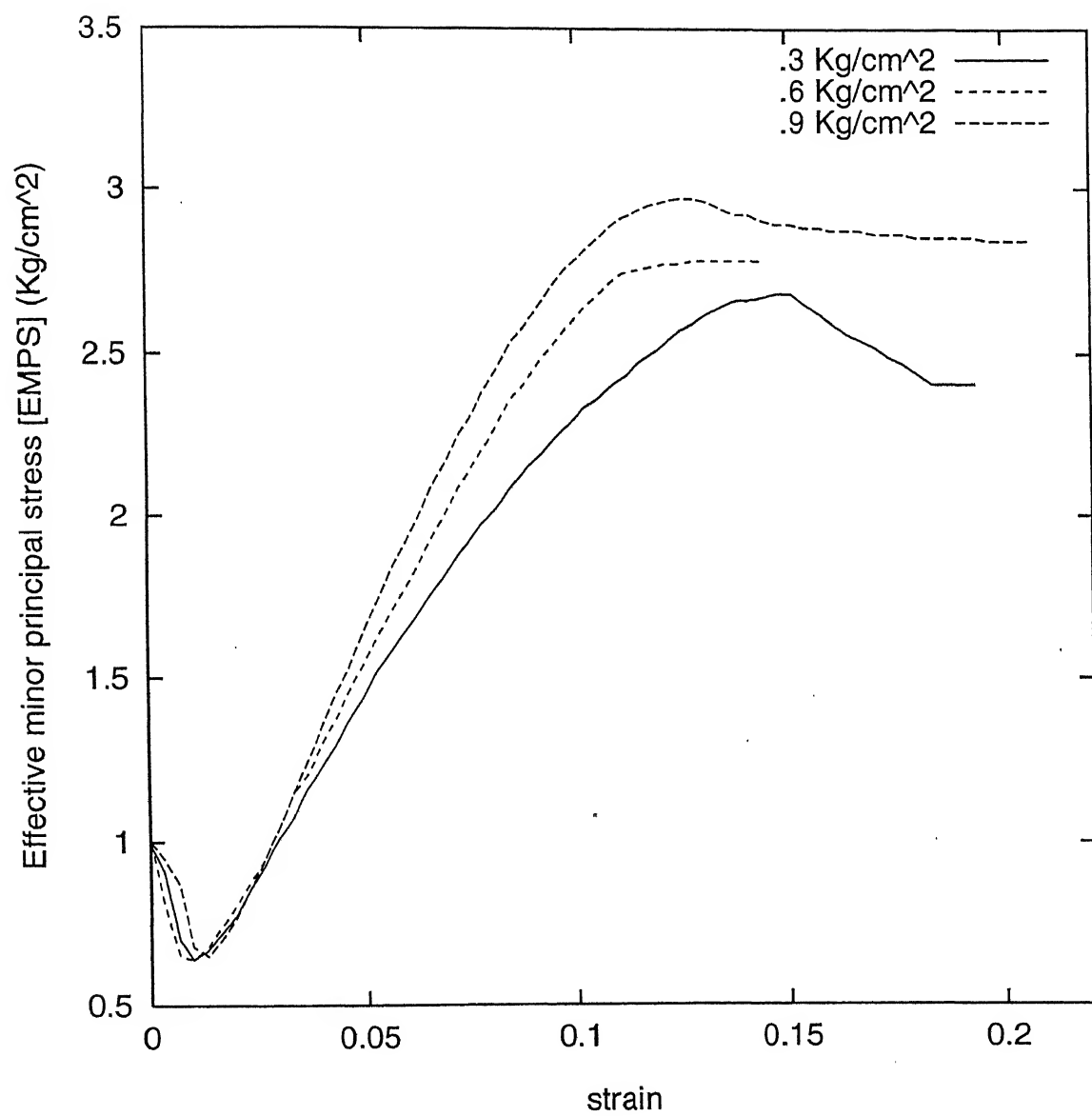


Fig. 3.16 Variation of [EMPS] with strain (STPP)

Table 3.3 S_{us} and void ratio for tube consolidated fly ash samples

Consolidation Pressure Kg./Cm ²	ϕ_s Degree	q_s Kg/Cm ²	Water Content After Test (%)	Void Ratio	S_{us} Kg/Cm ²	Effective Minor Principal Stress Kg/cm ²
--	--------------------	-----------------------------	--	---------------	--------------------------------	---

For STPP Fly Ash

.3	32.1	2.97	54.1	1.1	2.31	2.41
.6	34.0	3.52	52.6	1.08	2.92	2.78
.9	34.5	3.86	51.0	1.05	3.18	2.84

For HDTP Fly Ash

.6	31.2	2.52	53.2	1.055	2.16	2.34
.9	33.2	3.29	48.7	.944	2.75	2.72
1.2	33.4	3.47	47.3	.92	2.9	2.85

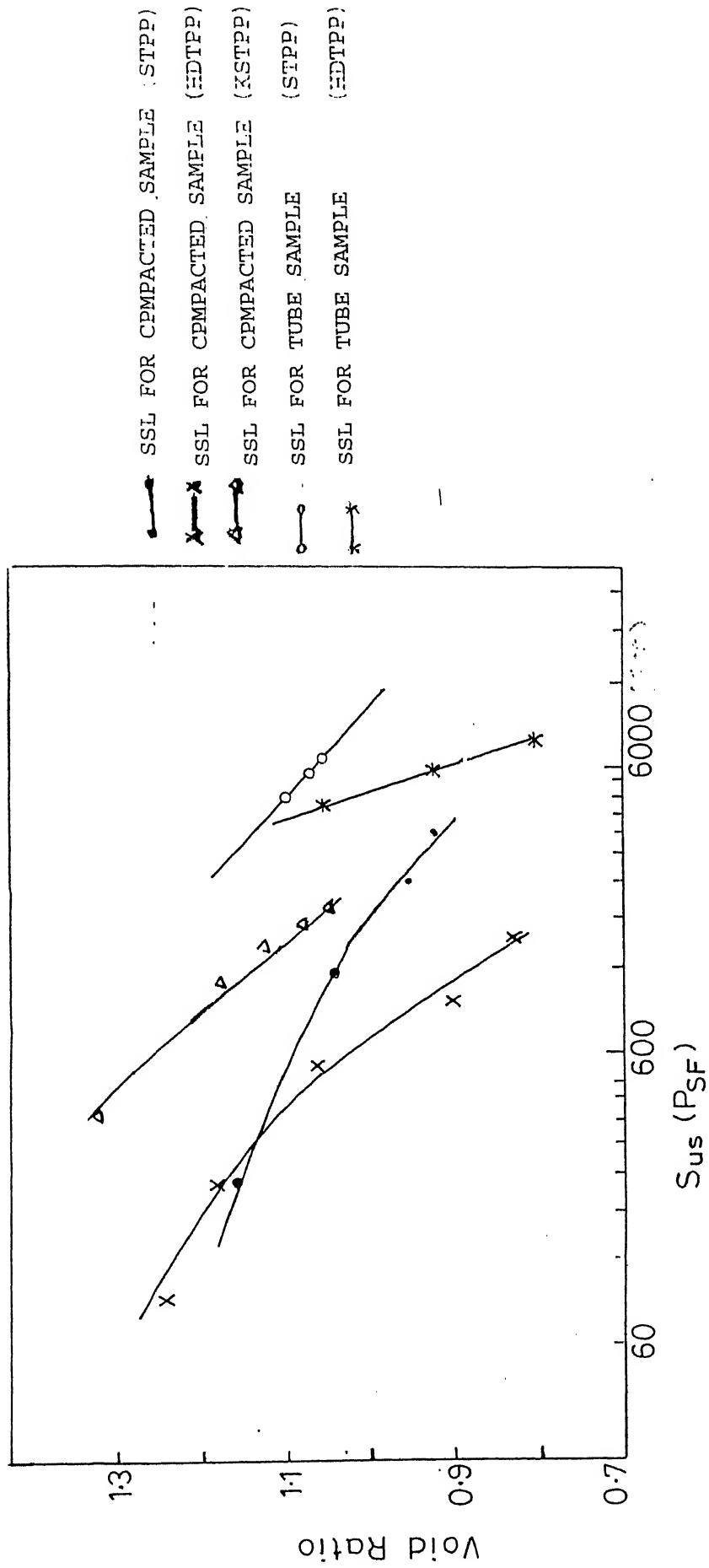


Fig. 3.17.2 Steady State Lines for STPP and HDTPP Fly-Ash

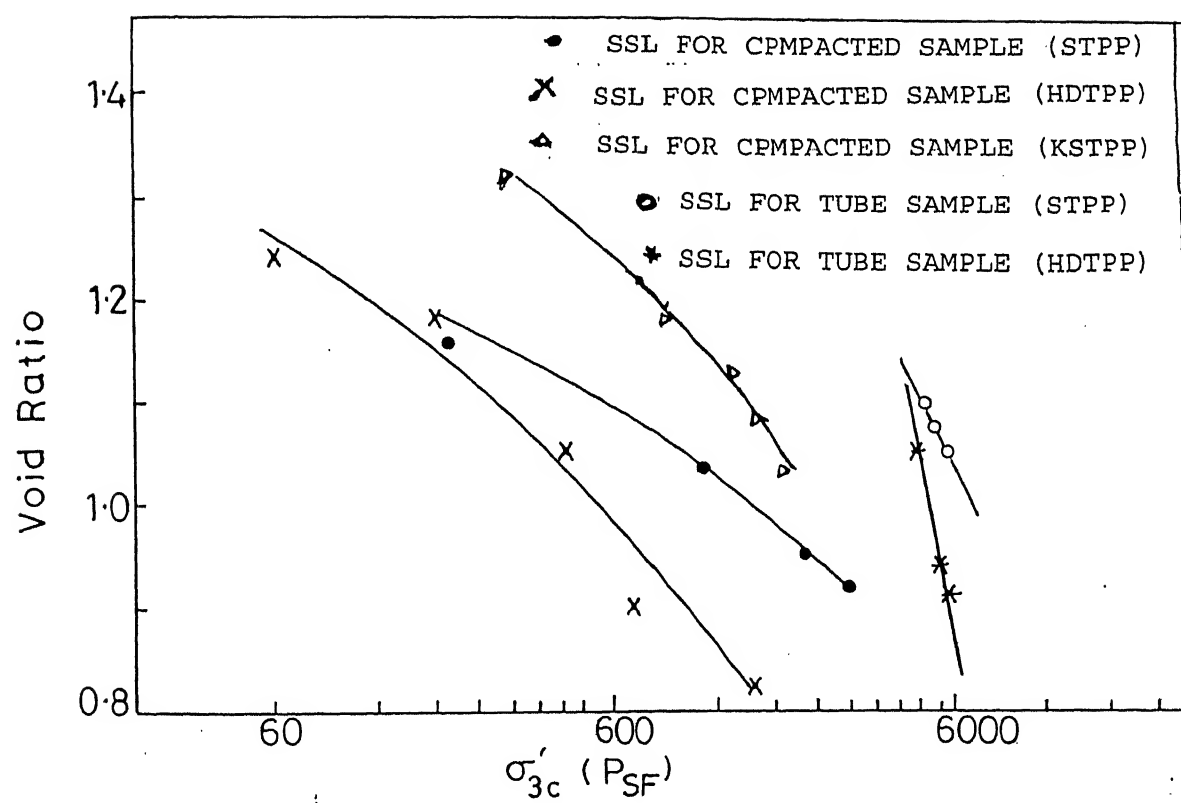


Fig.3.17(b) Steady State Lines for STPP and HDTTP Fly-Ash

CHAPTER 4

THEORETICAL ANALYSIS

4.1 General:

This chapter deals with the determination of S_{us} , shear modulus, and shear wave velocity at different depth.

4.2 Determination of steady state strength at different depth :

S_{us} value at field void ratio can be determined by correcting the S_{us} value of the undisturbed samples tested in the laboratory as explained in section 2.4.3.6 .Due to non availability of field samples here an attempt has been made to study the liquefaction phenomenon of tailings dam by interpolating results between the compacted dense samples and loose samples prepared in triaxial cell itself. Tube sample results as shown in Fig.3.13 & 3.15 of STPP and Fig. 3.14 & 3.16 of HDTPP clearly indicate the dilative behaviour and hence there is no possibility of liquefaction to occur in such types of samples. In the present analysis, therefore only the results of compacted and loose samples have been used.

As discussed in section 2.4.3 S_{us} value is function void ratio.

As the field void ratio at different depth is not presently available, it has been decided to get the corresponding field void ratio from the void ratio vs. consolidation pressure results of tube samples. As shown in Fig. 4.1 a straight line relationship is found between void ratio and log of octahedral consolidation pressure. For obtaining field void ratio first octahedral pressure

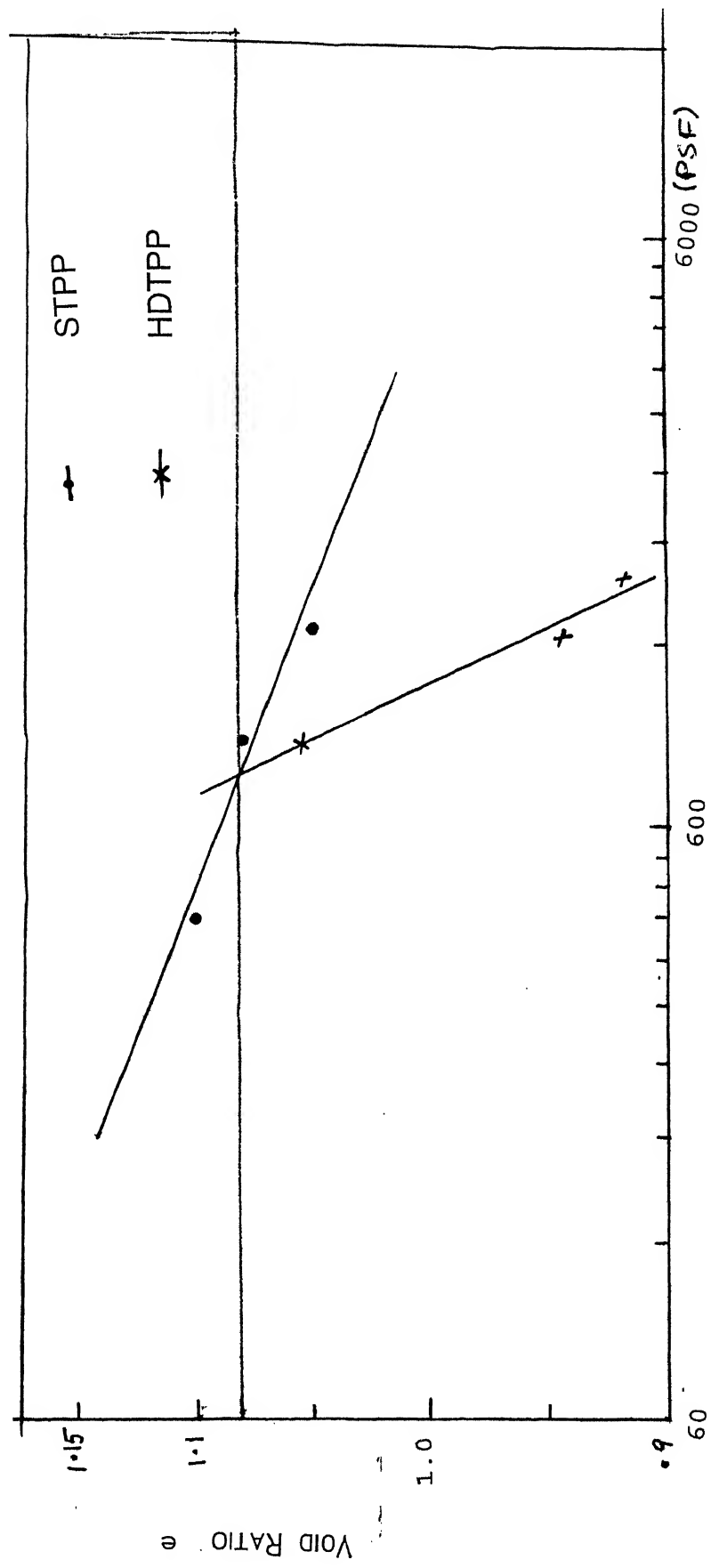


Fig. 4.1 VARIATION OF OCTAHEDRAL CONSOLIDATION PRESSURE VS. VOID RATIO

is determined at different depth using the correlation between effective stress and poission ratio as given in Eq. 4.1

$$\sigma_0 = \frac{(1+2\nu)\sigma'}{3} = \frac{2}{3}\sigma' \quad \text{Eq. 4.1}$$

σ_0 = Octahedral pressure

σ' = Effective Pressure

ν = Poission Ratio = .5 (Assumed)

From the octahedral pressure calculated at different depth, corresponding void ratio is determined by using Fig. 4.1. Using this void ratio the corresponding S_{us} value has been determined from SSL diagram of compacted and loose samples at different depths, from the Fig.3.17. The estimated S_{us} values at different depth is tabulated in Table 4.1 to 4.2 respectively, for STPP and HDTTP settled ash layers.

4.3 Determination of shear modulus shear wave velocity at different depth :

Shear modulus of soil at any depth can be calculated by using the formula given by Hardin-Black(1968), later modified by Christiano(1980), which is as follows :

$$G_{max} = \frac{17.760(2.973 - e)^2}{(1 + e)} (\sigma_0)^{0.5} \left(\frac{G}{2.7}\right)^2$$

Where :

G_{max} = Shear Modulus (KSF)

e = Void ratio

σ_0 = Octahedral pressure (PSF)

G = Specific Gravity

Shear wave velocity at any depth can be calculated by using the following formula :

$$V = \left(\frac{G_{max}}{\rho} \right)^{0.5}$$

Where :

V = Shear Wave Velocity

G_{max} = Shear Modulus

ρ = Mass Density

Void ratio as determined in section 4.2 is used to determine the shear modulus and shear wave velocity at different depth. Using the above formula shear modulus and shear wave velocity at different depth has been calculated and the results are given in Table 4.1 & Table 4.2 for STPP and HDTPP, respectively.

Table 4.1..Calculation of S_{us} Shear Modulus and shear wave velocity at different depth of embankment made of STPP Fly Ash

DEPTH	EFFECTIVE STRESS	OCTAHED-RAL PRESSURE	VOID RATIO	SHEAR MODULUS	SHEAR WAVE VEL.	S_{us}
m	σ' Kg/cm ²	σ_o Kg/cm ²	e	G_{max} Kg/cm ²	V m/Sec)	Kg/cm ²
0.760	0.106	0.070	0.920	102.063	85.042	1.67
3.048	0.337	0.225	0.920	182.332	194.194	1.67
5.334	0.409	0.273	1.093	154.641	186.404	0.293
6.096	0.440	0.293	1.090	161.110	190.263	0.299
7.620	0.502	0.334	1.084	173.486	197.436	0.336
9.144	0.563	0.375	1.079	185.220	204.004	0.352
10.668	0.624	0.416	1.075	196.410	210.075	0.368
12.192	0.686	0.457	1.071	207.131	215.733	0.395
13.716	0.747	0.498	1.067	217.442	221.038	0.413
15.240	0.808	0.539	1.063	227.391	226.038	0.423
16.760	0.870	0.580	1.060	237.018	230.773	0.443
18.288	0.931	0.621	1.057	226.352	235.273	0.453
19.812	0.993	0.662	1.055	255.423	239.565	0.464
21.336	1.054	0.703	1.052	264.254	243.671	0.486
22.860	1.115	0.744	1.049	272.863	247.609	0.508

Conversion Factor

$$1 \text{ Kg/Cm}^2 = 100 \text{ KN/m}^2$$

Table 4.2.Calculation of S_{us} ,Shear Modulus and shear wave velocity at different depth embankment made of HDTPP Fly Ash

DEPTH	EFFECTIVE STRESS	OCTAHED-RAL PRESSURE	VOID RATIO	SHEAR MODULUS	SHEAR WAVE VEL.	S_{us}
m	σ' Kg/cm ²	σ Kg/cm ²	e	G_{max} Kg/cm ²	V	Kg/cm ²
0.762	0.109	0.073	0.900	102.531	83.923	0.560
3.048	0.364	0.242	0.900	187.380	203.067	0.560
5.334	0.440	0.293	1.122	147.055	181.775	0.165
6.096	0.468	0.312	1.108	154.929	186.578	0.176
7.620	0.523	0.349	1.083	170.447	195.699	0.212
9.144	0.578	0.386	1.060	185.691	204.263	0.249
10.668	0.634	0.422	1.039	200.690	212.352	0.279
12.192	0.689	0.459	1.020	215.469	220.032	0.299
13.716	0.744	0.496	1.002	230.048	227.354	0.313
15.240	0.800	0.533	0.986	244.443	234.360	0.352
16.764	0.855	0.570	0.970	258.670	241.083	0.368
18.288	0.911	0.607	0.956	272.741	247.554	0.404
19.812	0.966	0.644	0.942	286.666	253.795	0.433
21.334	1.021	0.681	0.930	300.457	259.823	0.453
22.860	1.077	0.718	0.918	314.120	265.670	0.474

Conversion Factor

$$1 \text{ Kg/Cm}^2 = 100 \text{ KN/m}^2$$

CHAPTER 5

RESULTS AND DISCUSSION

5.1 General:

This chapter deals with liquefaction analysis of a typical ash embankments constructed by upstream method as shown in Fig. 5.1. For analysis geotechnical properties of STPP and HDTTP fly ashes, as discussed previously were used. The liquefaction analysis is carried out by empirical method, pseudo static method, steady state method, and simplified dynamic analysis following the procedures outlined in section 2.4 :- "Analysis of Uncompacted Embankment".

5.2 Ash Embankment details

Typically ash disposal dykes are constructed in several stages by "Upstream Method of Staged Construction" in five stages. As shown in Fig.5.1 a typical upstream constructed embankment consist of five to six stages and consist of three to four types of soils i. e. foundation soil, compacted earthen starter dam and compacted staged construction of earth or ash material and settled ash. In this analysis for the simplicity it has been assumed that the geotechnical properties of foundation soil and compacted earth dyke is same. The other two materials are ; compacted ash for stage II through stage V and settled lagoon ash. There are three types of soils assumed in this analysis are shown in Fig.5.1. Soil I is foundation and starter embankment soil, soil II is the compacted ash used in the construction of

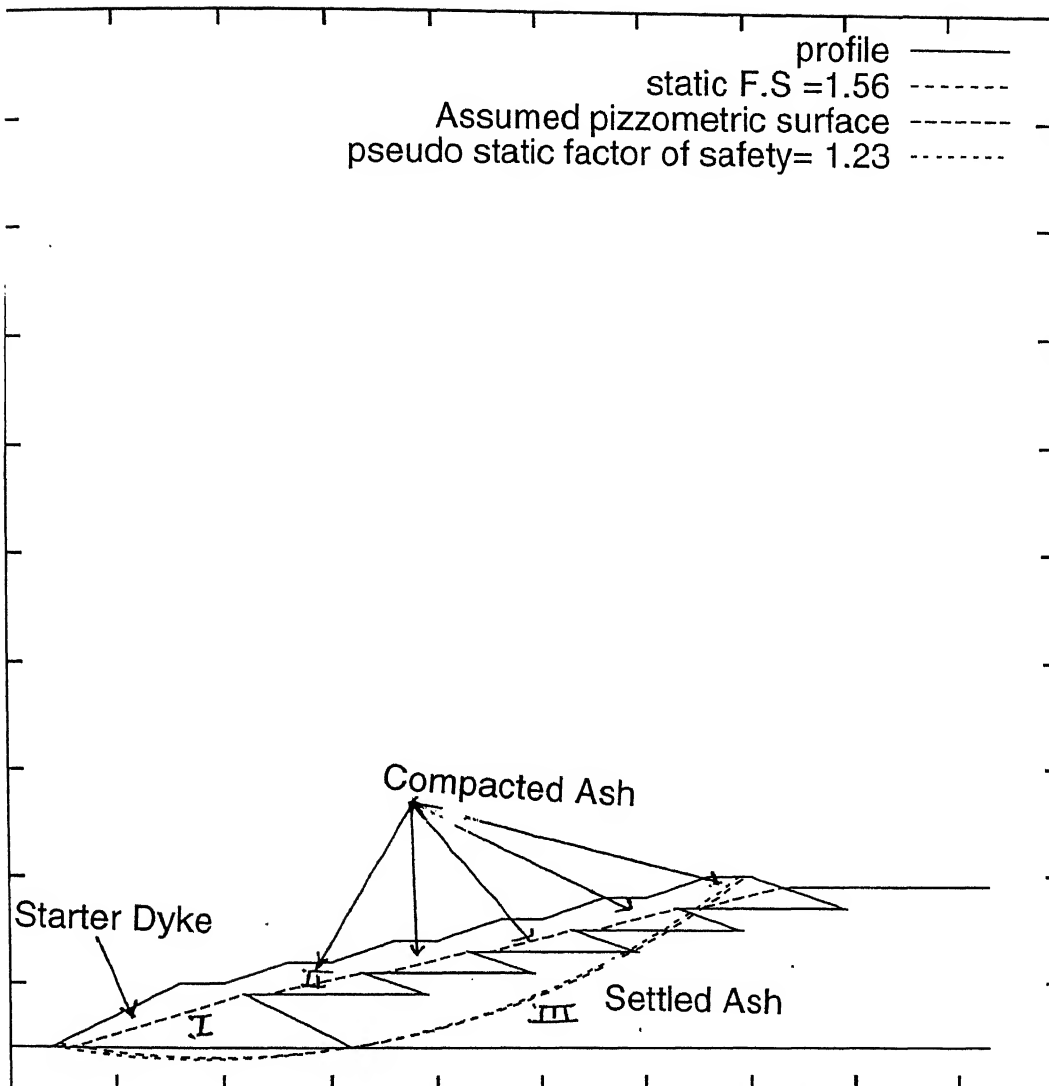


Fig. 5.1 Upstream method of Staged Construction

raising dykes and soil III is the settled Pond ash. The geotechnical properties used in the liquefaction analyses are summerized in the Table 5.1. These values are based on the test results and analysis as discussed in chapter 3 and chapter 4.

5.3 Liquefaction Analysis :

5.3.1 Empirical approach

As discussed in section 2.4.1.1, settlement of embankment depends on peak ground acceleration and earthquake magnitude. Different authors have given a correlation between peak ground acceleration and earthquake intensity as given in Table 5.2 .

According to seismic zonal map of India(I.S.1893 : 1984) both STPP and HDTPP sites fall somewhere in the range of seismic zone II and III. The modified Mercelli intensities assciated with zone II and III are 6 and 7, respectively and also the earthquake magnitude for zone II and III are of the same order.i.e 6 to 7. Earthquake magnitude of 6.5 is used here for the site under investigation.

The value of peak ground acceleration is calculated from various empirical formulae given in Table 5.3 and the results are summerized in the same Table ---. The ESI for each formula is calculated from the Eq. 2.1 and the percentage vertical settlement and horizontal movement are calculated from the relationship shown in Fig. 2.1. The absolute value of vertical settlement and horizontal movement for the configuration shown in Fig. 5.1 is also tabulated in the Table -. The range of vertical settlement is found to be .58 inch(1.46 cm.) to 1.92 inch(4.88 cm.)and the horizontal movement ranges from .25 inch(.62 cm.) to .91 inch(2.32

Table 5.1 : Geotechnical Properties of soil and Fly Ash used to carry out liquefaction analysis

Embankment Site HDTTP (KORBA WEST)

Geotechnical Properties	Soil Type		
	I	II	III
Specific Gravity	2.65	1.94	1.94
Moist Density	1.71	1.43	0.84 (Dry)
Saturated Density (gm/cc)	1.79	1.51	1.36
Shear strength Parametre			
Cohesion (C')	0	0	0
Effctive Friction Angle (ϕ')	30.0	31.5	26.0
Shear Modulus (KSF)	1000	Given in Table 4.2	
Shear Wave Velocity Ft/sec	800	Given in Table 4.2	

Embankment Site STPP (SARNI)

Geotechnical Properties	Soil Type		
	I	II	III
Specific Gravity	2.65	1.98	1.98
Moist Density	1.71	1.39	0.84 (Dry)
Saturated Density (gm/cc)	1.79	1.50	1.36
Shear strength Parametre			
Cohesion (C')	0	0	0
Effctive Friction Angle (ϕ')	30.0	35.5	26.0
Shear Modulus (KSF)	1000	Given in Table 4.1	
Shear Wave Velocity Ft/sec	800	Given in Table 4.1	

Table 5.3 - Deformation Calculation using Different Correlation as given in table 5.2

Empirical Relation	MMI = 6			MMI = 7		
	ESI	ΔH cm	ΔD cm	ESI	ΔH cm	ΔD cm
1	.264	1.47	1.10	.552	2.92	1.24
2	.520	2.69	1.27	1.064	4.88	2.44
3	.496	2.44	1.24	.992	4.39	2.18
4	.376	1.96	1.12	.848	4.24	1.96
5	.432	2.21	1.17	1.024	4.60	2.26
6	.456	2.32	1.19	.816	3.91	1.91

cm.). It is to be noted that for the most conservative correlation by (Neumann 1954), the maximum settlement is found to be 1.92 inch(4.88 cm.).

5.3.2 Pseudo Static analysis:

Before carrying out the pseudo static analysis static stability analysis has been carried out to see whether it is statically safe or not.

The seismic stability analysis is performed for pseudo static condition assuming suitable earthquake loading. The recommendations published by the Indian Standard (IS 1893 : 1984) suggest that a seismic acceleration of .05g acting in the horizontal direction may be used for the site. The factor of safety for static and dynamic condition are shown in Fig. 5.1 PCSTABL5; a software package has been used for both static and seismic analysis which has been discussed in section 2.6. Using modified Bishop method, it has been found that the static factor of safety is 1.56 and 1.54 for STPP and HDTPP dyke site, respectively which is more than the required F.S. of 1.5 whereas under pseudo static condition factor of safety is 1.23 and 1.225 for STPP and HDTPP dyke site, respectively. Various international agencies have suggested that under pseudo static condition factor of safety should be of the order of 1 to 1.2. Computer print out for STPP dyke site has been given in the appendix.

After ensuring that the dam is safe for both static and pseudo static conditions, further analysis has been carried out, assuming different values of horizontal acceleration to get a factor of safety of equal to one which indicates that the dam is

unsafe for acceleration value higher than that at which factor of safety is one. It has been found that ash embankments both STPP and HDTPP are safe up to 0.11 g horizontal acceleration.

5.3.3 Steady State Method:

In this method driving shear stress is determined using the undrained soil property of uncompacted ash. Driving shear stress is determined by trial and error using PCSTABL5 program for modified bishop method to obtain a factor of safety equal to one. Using a number of iteration it has been found that the driving stress for ash embankment at STPP site is 170 PSF and that of HDTPP site it is 175 PSF. From table 4.1 and 4.2, the minimum value of S_{us} is 600 PSF and 337 PSF for STPP and HDTPP which is much more than the driving shear stress. Hence there is no possibility of liquefaction to occur. The actual F.S.= 1.32 has been found for HDTPP dyke siteout from PCSTABL5 program for modified Bishop's failure circles by substituting S_{us} values of various layers of 10 ft. (3.05 m increments). As it has already been discussed in the section 2.4.3 that S_{us} value is very sensitive to void ratio, this result is not very much satisfactory due to non availability of field void ratio. Nevertheless an attempt has been made to demonstrate, how the steady state method could be used for investigation of liquefaction potential of a fly ash dyke constructed by upstream method.

5.3.4 Simplified Dynamic analysis:

This analysis is another approach for assessing the liquefaction potential of a dam/tailing dams. In this method,

yield acceleration(K_y), maximum average acceleration due to earthquake (K_{max}) and time period (T_o) are obtained and from those results the maximum deformation of embankment is determined.

As discussed in section 2.4.4.2, yield acceleration (K_y) is the horizontal acceleration for which embankment has a factor of safety equal to one. This is calculated by pseudo static method as discussed in the section 5.3.2.

Maximum average acceleration and time period induced due to earthquake is determined using 'SHAKE' program for Pasadena and Kern Taft earthquake records. The reason for selecting the above earthquake records, is that the acceleration spectrum of these earthquake records are for medium dense soil. Similar one found at STTP and HDTPP sites. In order to calculate acceleration at different depth (to simulate earthquake condition) horizontal motion of $0.15g$ is given at the base of the embankment and induced acceleration at different depth is determined by using 'SHAKE' program. It also gives the value of first natural period. As discussed in section 2.4.4.3, the maximum average acceleration is determined by averaging the maximum acceleration from top of the embankment to the depth at which failure circle passes. The average of these values gives the K_{max} value. Knowing the value of K_y/K_{max} and T_o (time period) maximum deformation of the embankment is calculated using the procedure outline in section 2.4.4. After knowing the total deformation of the embankment one can decide whether it is permissible or exceeding the limits.

The shake analysis result is given in the appendix. The deformation analysis is carried out for three different heights of the embankment, 60ft (18.29 m), 70 ft. (21.34m) and 80ft (24.38 m)

for both sites .The results are shown in the Table 5.3. As shown in the table for 80 ft.(24.38 m), the maximum deformation from this method is found to be 1.07 inch(2.72 cm) for HDTPP site and 1.2 inch (3.05 cm)for STPP site. As mentioned in the section 5.3.1, the deformation from empirical relation is found to vary between 1.92 inch (4.88 cm) inch to 0.58 inch(1.47 cm.) inch which is very comparable to those obtained for simplified dynamic analysis. One sample computer printout for HDTPP dyke site has been given in the appendix .

Table 5.4 Deformation calculation for embankment made by HDTTP

Ash sample

Embankment height m	Time Period (Sec)		K _{max}		K _y	K _y /K _{max}		U _{max} K _{max} gTo		U _{max} Cm.	
	K	P	K	P		K	P	K	P	K	P
24.38	.94	1.24	.188	.186	.11	.585	.59	.013	.012	2.26	2.72
21.34	.91	1.22	.165	.170	.11	.667	.647	.006	.008	0.89	1.63
18.29	.86	1.19	.157	.167	.11	.701	.659	.005	.007	0.66	1.37

Deformation calculation for embankment made by STPP

Ash sample

Embankment height m	Time Period (Sec)		K _{max}		K _y	K _y /K _{max}		U _{max} K _{max} gTo		U _{max} Cm.	
	K	P	K	P		K	P	K	P	K	P
24.38	.98	1.29	.183	.185	.11	.601	.595	.014	.012	2.11	3.05
21.34	.94	1.27	.167	.171	.11	.659	.643	.007	.007	1.07	1.78
18.29	.89	1.22	.157	.164	.11	.701	.671	.005	.005	0.69	1.12

K stands for Kerntaft earthquake record

P stands for Pasadena earthquake record

U_{max} - Settlement.

CHAPTER 6

CONCLUSIONS

In this investigation, liquefaction evaluation was carried out for two ash disposal sites satpura Thermal power plant (STPP) Sarni, and Hansdeo Thermal Power Plant(HDTPP) Korba West, located in Madhya pradesh. The essential geotechnical tests such as grain size distribution, specific gravity, standard procter test, triaxial test with pore pressure measurements and S_{us} test were performed which are required for the liquefaction analysis .

The liquefaction analysis of a tailings dam is generally performed by empirical method, pseudo static method, steady state method, simplified liquefaction analysis and complete dynamic analysis. In this investigation, liquefaction analysis is carried out by first four method as stated above and the evaluation procedures and findings are summarized below:

(1) Empirical analysis was performed based on the Earthquake Severity Index (ESI) procedure as outlined by ICOLD applicable for earthquake zone of the site and typical upstream embankment configuration. Range of vertical deformation by this method is found to vary between 1.92 inch. (4.876 cm) and 0.58 inch. (1.467cm) and the horizontal movement between .34 inch (.85 cm) to .96 inch (2.44 cm) .

(2) pseudo-static analysis was carried out as per the recommendation given in I.S.1893:1984. Factor of safety equal to 1.23 is found for horizontal seismic coefficient of 0.05g which is recommended by I.S.1893 :1984.

(3) In steady state method, consolidated undrained test with pore pressure measurement were performed on samples compacted at 85 %, 90 % , 95% and 100% standard Procter density and on a very loose

samples and the void ratio versus S_{us} relationship were established. settled ash slurry tube samples were prepared in the laboratory at various consolidation pressure simulating the field conditions and a relationship between void ratio versus consolidation pressure was established. The void ratio at different depth in a settled ash is estimated based on octahedral consolidation pressure likely to be developed in different layers of settled ash and corresponding to that pressure, void ratio were determined from the tube sample results. The corresponding S_{us} values were determined from S_{us} versus void ratio relationship. Liquefaction analysis was carried out and embankment is found to be safe against liquefaction for five stages of upstream construction. The factor of safety is found to be 1.32 for HDTPP dyke site.

(4) Simplified dynamic analysis was carried out using SHAKE program. Shear modulus and shear wave velocity were determined using the standard correlation using the laboratory test results. Maximum deformation of the five staged embankment constructed by upstream method of staged construction is 1.07 inch (2.72 cm) for HDTPP site and 1.2 inch (3.05 cm) for STPP site.

Recommendation for Further Investigations:

Due to the logistic problem and time limitations undisturbed sample could not be obtained from test sites. In this investigation entire exercise is carried out simulating field conditions in the laboratory. as discussed in the chapter two, the steady state undrained shear test strength and shear wave velocity are very susceptible to void ratio. It is therefore recommended

that similar investigations as presented here may be carried out on high quality of undisturbed samples obtained at various depth from ash lagoons. Complete dynamic analysis utilizing the finite element technique should also be persued with actual soil dynamic properties obtained from the ash lagoon sites.

S H A K E S

A program for:

Earthquake Response Analysis
of Horizontally Layered Sites
Version of February 1988

Originally authored by
Schnabel, Lysmer, & Seed
Modified by J. Sun & S. Lai
University of California - Berkeley

IBM-PC version by
Geotech International
(312) 939-7162
May 1991

Input file name = kbn80k.in
Output file name = kbn80k.ot
Punch file name = fds

Date and time of run = 1/01/1980 9:47

MAX. NUMBER OF TERMS IN FOURIER TRANSFORM = 4096
NECESSARY LENGTH OF BLANK COMMON X = 25619
EARTH PRESSURE AT REST FOR SAND = .500

1***** OPTION 8 *** READ RELATION BETWEEN SOIL PROPERTIES AND STRAIN

CURVES FOR RELATION OF STRAIN VERSUS SHEAR MODULUS AND DAMPING

MODULUS AND DAMPING VALUES ARE SCALED FOR PLOTTING

SHEAR MODULUS CLAY - MAY 1972	MULTIPLICATION FACTOR = .01000
DAMPING CLAY - MAY 24, 1972	MULTIPLICATION FACTOR = 1.00000
SHEAR MODULUS SAND SQ.ROOT REL. - MAY 1972	MULTIPLICATION FACTOR = .50000
DAMPING SAND - FEBRUARY 1971	MULTIPLICATION FACTOR = 1.00000
ATTENUATION OF ROCK AVERAGE 9/4	MULTIPLICATION FACTOR = .01000
DAMPING IN ROCK AVERAGE 9/4	MULTIPLICATION FACTOR = 1.00000
C1 (CLAY PI = 0-10) MODULUS REDUCTION CURVES, FEB 1988	MULTIPLICATION FACTOR = 30.00000
DAMPING CLAY - MAY 24, 1972	MULTIPLICATION FACTOR = 1.00000
C2 (CLAY PI = 10-20) MODULUS REDUCTION CURVES, FEB 1988	MULTIPLICATION FACTOR = 30.00000
DAMPING CLAY - MAY 24, 1972	MULTIPLICATION FACTOR = 1.00000
C3 (CLAY PI = 20-40) MODULUS REDUCTION CURVES, FEB 1988	MULTIPLICATION FACTOR = 30.00000
DAMPING CLAY - MAY 24, 1972	MULTIPLICATION FACTOR = 1.00000
C4 (CLAY PI = 40-60) MODULUS REDUCTION CURVES, FEB 1988	MULTIPLICATION FACTOR = 30.00000
DAMPING CLAY - MAY 24, 1972	MULTIPLICATION FACTOR = 1.00000
C5 (CLAY PI > 60) MODULUS REDUCTION CURVES, FEB 1988	MULTIPLICATION FACTOR = 30.00000
DAMPING CLAY - MAY 24, 1972	MULTIPLICATION FACTOR = 1.00000
S1 (SAND CP=.25 KSC) MODULUS REDUCTION CURVES, FEB 1988	MULTIPLICATION FACTOR = 30.00000
DAMPING SAND - FEBRUARY 1971	MULTIPLICATION FACTOR = 1.00000
S2 (SAND CP=.50 KSC) MODULUS REDUCTION CURVES, FEB 1988	MULTIPLICATION FACTOR = 30.00000
DAMPING SAND - FEBRUARY 1971	MULTIPLICATION FACTOR = 1.00000
S3 (SAND CP=1.0 KSC) MODULUS REDUCTION CURVES, FEB 1988	MULTIPLICATION FACTOR = 30.00000


```

100000  OPTION 1 *** READ INPUT MOTION
EARTHQUAKE - VERN COUNTY TAFT 7/21/52.58PE
2720 ACCELERATION VALUES AT TIME INTERVAL .0200
THE VALUES ARE LISTED ROW BY ROW AS READ FROM CARDS
TRAILING ZEROS ARE ADDED TO GIVE A TOTAL OF 4096 VALUES
MAXIMUM ACCELERATION = 17.526
AT TIME = 3.10 SEC
THE VALUES WILL BE MULTIPLIED BY A FACTOR = .840
TO GIVE NEW MAXIMUM ACCELERATION = .15067
MEAN SQUARE FREQUENCY = 2.75 C/SEC
100000  OPTION 2 *** READ SOIL PROFILE
NEW SOIL PROFILE NO. 1 IDENTIFICATION - Sarni pond ash
NUMBER OF LAYERS 10 DEPTH TO BEDROCK 80.00
NUMBER OF FIRST SUBMERGED LAYER 2 DEPTH TO WATER LEVEL 5.00

```

LAYER	TYPE	FACTOR	THICKNESS FT	DEPTH FT	EFF. PRESS. KSF	MODULUS KSF	DAMPING	UNIT WEIGHT KCF	SHEAR VEL FT/SEC
1	10	1.00	5.00	2.50	.21	210.	.050	.0820	237.
2	10	1.00	10.00	19.99	.26	384.	.050	.0320	622.
3	9	1.00	5.00	17.50	.02	302.	.050	.0260	611.
4	9	1.00	10.00	25.00	.26	350.	.050	.0260	658.
5	9	1.00	10.00	35.00	.62	412.	.050	.0260	714.
6	9	1.00	10.00	45.00	.79	412.	.050	.0260	764.
7	9	1.00	10.00	55.00	-1.35	531.	.050	.0260	811.
8	9	1.00	10.00	65.00	-1.71	589.	.050	.0260	853.
9	9	1.00	10.00	75.00	-2.08	644.	.050	.0260	892.
10	BASE					1000.			

PERIOD = 44 FROM AVERAGE SHEAR VELOCITY = 721. FT/SEC

MAXIMUM AMPLIFICATION = 12.93
FOR FREQUENCY = 2.12 C/SEC.
PERIOD = .47 SEC

1***** OPTION 3 *** READ WHERE OBJECT MOTION IS GIVEN

OBJECT MOTION IN LAYER NUMBER 9 WITHIN

1***** OPTION 4 *** OBTAIN STRAIN COMPATIBLE SOIL PROPERTIES

MAXIMUM NUMBER OF ITERATIONS = 7
 MAXIMUM ERROR IN PERCENT = 5.00
 FACTOR FOR EFFECTIVE STRAIN IN TIME DOMAIN = .05

EARTHQUAKE - KERN COUNTY, TAFT, 7/21/52, S65E
 SOIL PROFILE - Sarni Pond ash

ITERATION NUMBER 1

THE CALCULATION HAS BEEN CARRIED OUT IN THE TIME DOMAIN WITH EFF. STRAIN = .65* MAX. STRAIN

LAYER TYPE	DEPTH FT	EFF. STRAIN PRCNT	NEW DAMP	DAMP USED	ERROR PRCNT	NEW C KSF	C USED KSF	ERROR PRCNT
1 10	2.5	.03296	.109	.050	53.6	112.039	210.300	-87.7
2 10	10.0	.05741	.127	.050	60.6	171.104	384.300	-124.6
3 9	17.5	.07325	.153	.050	67.4	76.319	331.600	-295.2
4 9	25.0	.10350	.155	.050	67.9	85.833	349.600	-307.3
5 9	32.5	.10576	.157	.050	68.2	99.389	411.600	-314.1
6 9	40.0	.12526	.157	.050	69.1	114.561	471.800	-311.8
7 9	47.5	.10121	.155	.050	67.7	131.795	530.500	-302.5
8 9	55.0	.09478	.151	.050	67.0	153.545	587.900	-282.9
9 9	75.0	.09743	.147	.050	66.1	179.071	644.200	-259.7

VALUES IN TIME DOMAIN

LAYER TYPE	THICKNESS FT	DEPTH FT	MAX STRAIN PRCNT	MAX STRESS PSF	TIME SEC
1 10	5.0	2.5	.05993	67.15	8.20
2 10	10.0	10.0	.09633	151.13	8.20
3 9	5.0	17.5	.15161	115.71	7.78
4 9	10.0	25.0	.15923	136.67	8.00
5 9	10.0	32.5	.15425	163.25	8.00
6 9	10.0	40.0	.18256	156.23	8.00
7 9	10.0	47.5	.15570	205.21	8.00
8 9	10.0	55.0	.14531	223.89	8.00
9 9	10.0	75.0	.13452	240.98	8.00

EARTHQUAKE - KERN COUNTY, TAFT, 7/21/52, S65E
 SOIL PROFILE - Sarni Pond ash

ITERATION NUMBER 2

THE CALCULATION HAS BEEN CARRIED OUT IN THE TIME DOMAIN WITH EFF. STRAIN = .65* MAX. STRAIN

LAYER TYPE	DEPTH FT	EFF. STRAIN PRCNT	NEW DAMP	DAMP USED	ERROR PRCNT	NEW C KSF	C USED KSF	ERROR PRCNT
1 10	2.5	.02452	.028	.108	-22.2	130.778	112.039	14.3
2 10	10.0	.04331	.114	.127	-11.6	194.357	171.104	12.0
3 9	17.5	.11272	.155	.122	7.1	53.912	76.319	-19.1

5	9	10.0	35.0	.22579	196.14	6.22
6	9	10.0	45.0	.17084	190.50	6.80
7	9	10.0	55.0	.11698	190.56	6.78
8	9	10.0	65.0	.09401	194.88	7.30
9	9	10.0	75.0	.08185	201.14	7.28

1 EARTHQUAKE - KERN COUNTY, TAFT, 7/21/52, S69E
SOIL PROFILE - Sarni pond ash

ITERATION NUMBER 6

THE CALCULATION HAS BEEN CARRIED OUT IN THE TIME DOMAIN WITH EFF. STRAIN = .65* MAX. STRAIN

LAYER	TYPE	DEPTH FT	EFF. STRAIN PRCNT	NEW DAMP.	DAMP USED	ERROR PRCNT	NEW G KSF	G USED KSF	ERROR PRCNT
1	10	2.5	.01882	.079	.079	-1	139.979	139.937	.0
2	10	10.0	.03257	.099	.099	-4	220.274	219.486	.4
3	9	17.5	.17686	.183	.180	1.1	52.980	54.591	-3.0
4	9	25.0	.17877	.183	.181	1.0	60.923	62.603	-2.8
5	9	35.0	.14830	.174	.173	.2	81.755	82.075	-4
6	9	45.0	.10892	.158	.159	-6	112.696	111.504	1.1
7	9	55.0	.07153	.138	.141	-2.2	169.660	162.904	4.0
8	9	65.0	.05857	.128	.130	-1.6	212.496	207.305	2.4
9	9	75.0	.05180	.122	.123	-1.1	249.336	245.746	1.4

VALUES IN TIME DOMAIN

LAYER	TYPE	THICKNESS FT	DEPTH FT	MAX STRAIN PRCNT	MAX STRESS PSF	TIME SEC
1	10	5.0	2.5	.02895	40.52	3.90
2	10	10.0	10.0	.05011	110.37	6.82
3	9	5.0	17.5	.27209	144.15	6.82
4	9	10.0	25.0	.27503	167.56	6.82
5	9	10.0	35.0	.22815	185.52	6.82
6	9	10.0	45.0	.16757	188.84	6.80
7	9	10.0	55.0	.11004	165.70	6.78
8	9	10.0	65.0	.09011	191.47	7.30
9	9	10.0	75.0	.07969	152.69	7.28

PERIOD = .80 FROM AVERAGE SHEAR VELOCITY = 401. FT/SEC

MAXIMUM AMPLIFICATION = 3.97
FOR FREQUENCY = 1.07 C/SEC.
PERIOD = .94 SEC.

***** OPTION 5 *** COMPUTE MOTION IN NEW SUBLAYERS

EARTHQUAKE - KERN COUNTY, TAFT, 7/21/52, S69E
SOIL DEPOSIT - Sarni pond ash

LAYER	DEPTH FT	MAX. ACC. G	TIME SEC	MEAN SQ. FR. C/SEC	ACC. RATIO QUIET ZONE	PUNCHED CARDS ACC. RECORD
WITHIN	0	.19717	3.90	1.51	.001	1
OUT	2	.19008	1.90	1.44	.002	1

5	9	10.0	35.0	.22679	126.14	6.82
6	9	10.0	45.0	.17084	190.50	6.80
7	9	10.0	55.0	.11698	190.56	6.78
8	9	10.0	65.0	.09401	194.88	7.30
9	9	10.0	75.0	.08125	201.14	7.28

1 EARTHQUAKE - KERN COUNTY, TAFT, 7/21/52, S69E
SOIL PROFILE - Sarni pond ash

ITERATION NUMBER 6

THE CALCULATION HAS BEEN CARRIED OUT IN THE TIME DOMAIN WITH EFF. STRAIN = .65* MAX. STRAIN

LAYER	TYPE	DEPTH FT	EFF. STRAIN PRCNT	NEW DAMP.	DAMP USED	ERROR PRCNT	NEW G KSF	G USED KSF	ERROR PRCNT
1	10	2.5	.01882	.079	.079	-.1	139.979	139.937	.0
2	10	10.0	.03257	.099	.099	-.4	220.274	219.486	.4
3	9	17.5	.17686	.183	.180	1.1	52.980	54.591	-3.0
4	9	25.0	.17877	.183	.181	1.0	60.923	62.603	-2.8
5	9	35.0	.14830	.174	.173	.2	81.755	82.075	-.4
6	9	45.0	.10892	.158	.159	-.6	112.696	111.504	1.1
7	9	55.0	.07153	.138	.141	-2.2	169.660	162.904	4.0
8	9	65.0	.05857	.128	.130	-1.6	212.496	207.305	2.4
9	9	75.0	.05180	.122	.123	-1.1	249.336	245.746	1.4

VALUES IN TIME DOMAIN

LAYER	TYPE	THICKNESS FT	DEPTH FT	MAX STRAIN PRCNT	MAX STRESS PSF	TIME SEC
1	10	5.0	2.5	.02895	40.52	3.90
2	10	10.0	10.0	.05011	110.37	6.82
3	9	5.0	17.5	.27209	144.16	6.82
4	9	10.0	25.0	.27503	167.56	6.82
5	9	10.0	35.0	.22815	186.52	6.82
6	9	10.0	45.0	.16757	188.84	6.80
7	9	10.0	55.0	.11004	186.70	6.78
8	9	10.0	65.0	.09011	191.47	7.30
9	9	10.0	75.0	.07969	198.69	7.28

PERIOD = .80 FROM AVERAGE SHEAR VELOCITY = 401. FT/SEC

MAXIMUM AMPLIFICATION = 3.97
FOR FREQUENCY = 1.07 C/SEC.
PERIOD = .94 SEC.

1***** OPTION 5 *** COMPUTE MOTION IN NEW SUBLAYERS

EARTHQUAKE - KERN COUNTY, TAFT, 7/21/52, S69E
SOIL DEPOSIT - Sarni pond ash

LAYER	DEPTH FT	MAX. ACC. G	TIME SEC	MEAN SQ. FR. C/SEC	ACC. RATIO QUIET ZONE	PUNCHED CARDS ACC. RECORD
WITHIN	.0	.19717	3.90	1.51	.001	1

WITHIN	15.0	.17788	6.80	1.30	.003	1
WITHIN	20.0	.14554	6.78	1.56	.001	1
WITHIN	30.0	.10785	4.66	2.59	.002	1
WITHIN	40.0	.15915	3.76	2.79	.002	1
WITHIN	50.0	.15997	3.74	2.87	.001	1
WITHIN	60.0	.15378	3.72	2.90	.002	1
WITHIN	70.0	.15087	3.70	2.97	.002	1
WITHIN	80.0	.14819	3.68	3.11	.001	1

 Total execution time = 7.0 mins

**** PCSTABLES ****

by
Purdue University

--Slope Stability Analysis--
Simplified Janbu, Simplified Bishop
or Spencer's Method of Slices

Run Date:
Time of Run:
Run By:
Input Data Filename: k2.in
Output Filename: k2.ot

PROBLEM DESCRIPTION PCSTABLES Example Problem (Sarni STPP)

BOUNDARY COORDINATES

15 Top Boundaries
31 Total Boundaries

Boundary No.	X-Left (ft)	Y-Left (ft)	X-Right (ft)	Y-Right (ft)	Soil Type Below Bnd
1	.00	20.00	20.00	20.00	1
2	20.00	20.00	80.00	50.00	1
3	80.00	50.00	100.00	50.00	1
4	100.00	50.00	130.00	60.00	2
5	130.00	60.00	150.00	60.00	2
6	150.00	60.00	180.00	70.00	2
7	180.00	70.00	200.00	70.00	2
8	200.00	70.00	230.00	80.00	2
9	230.00	80.00	250.00	80.00	2
10	250.00	80.00	280.00	90.00	2
11	280.00	90.00	300.00	90.00	2
12	300.00	90.00	330.00	100.00	2
13	330.00	100.00	350.00	100.00	2
14	350.00	100.00	365.00	95.00	2
15	365.00	95.00	465.00	95.00	3
16	365.00	95.00	395.00	85.00	2
17	300.00	90.00	315.00	85.00	2
18	315.00	85.00	395.00	85.00	3
19	315.00	85.00	345.00	75.00	2
20	265.00	75.00	345.00	75.00	3
21	265.00	75.00	295.00	65.00	2
22	200.00	70.00	215.00	65.00	2
23	315.00	65.00	295.00	65.00	3
24	215.00	65.00	245.00	55.00	2
25	150.00	60.00	165.00	55.00	2
26	165.00	55.00	245.00	55.00	3
27	165.00	55.00	195.00	45.00	2
28	100.00	50.00	110.00	45.00	1
29	110.00	45.00	195.00	45.00	3
30	110.00	45.00	160.00	20.00	1
31	20.00	20.00	400.00	20.00	1

ISOTROPIC SOIL PARAMETERS

3 Type(s) of Soil

Soil Type No.	Total Unit Wt. (pcf)	Saturated Unit Wt. (pcf)	Cohesion Intercept (psf)	Friction Angle (deg)	Pore Pressure Param.	Pressure Constant (psf)	Piez. Surface No.
1	107.0	112.0	.0	30.0	.00	.0	1
2	91.0	96.0	.0	35.5	.00	.0	1
3	80.0	85.0	.0	26.0	.00	.0	1

1 PIEZOMETRIC SURFACE(S) HAVE BEEN SPECIFIED

Unit Weight of Water = 62.40

Piezometric Surface No. 1 Specified by 14 Coordinate Points

Point No.	X-Water (ft)	Y-Water (ft)
1	20.00	20.00
2	30.00	20.00
3	110.00	45.00
4	130.00	45.00
5	165.00	55.00
6	185.00	55.00
7	215.00	65.00
8	235.00	65.00
9	265.00	75.00
10	285.00	75.00
11	315.00	85.00
12	335.00	85.00
13	375.00	95.00
14	465.00	95.00

A Critical Failure Surface Searching Method, Using A Random Technique For Generating Circular Surfaces, Has Been Specified.

100 Trial Surfaces Have Been Generated.

10 Surfaces Initiate From Each Of 10 Points Equally Spaced Along The Ground Surface Between X = 10.00 ft.
and X = 30.00 ft.

Each Surface Terminates Between X = 330.00 ft.
and X = 350.00 ft.

Unless Further Limitations Were Imposed, The Minimum Elevation

At Which A Surface Extends Is Y = .00 ft.

8.00 ft. Line Segments Define Each Trial Failure Surface.

Following Are Displayed The Ten Most Critical Of The Trial Failure Surfaces Examined. They Are Ordered - Most Critical First.

* * Safety Factors Are Calculated By The Modified Bishop Method * *

Failure Surface Specified By 44 Coordinate Points

Point No.	X-Surf (ft)	Y-Surf (ft)
1	23.33	21.67
2	31.23	20.36
3	39.14	19.20
4	47.08	18.19
5	55.03	17.34
6	63.00	16.64
7	70.98	16.09
8	78.97	15.70
9	86.97	15.45
10	94.97	15.36
11	102.97	15.43
12	110.97	15.64
13	118.96	16.01
14	126.94	16.54
15	134.91	17.21
16	142.87	18.04
17	150.81	19.02
18	158.73	20.15
19	166.62	21.44
20	174.49	22.87
21	182.34	24.46
22	190.15	26.19
23	197.92	28.08
24	205.66	30.11
25	213.36	32.29
26	221.01	34.62
27	228.62	37.09
28	236.18	39.71
29	243.68	42.47
30	251.14	45.38
31	258.53	48.43
32	265.87	51.61
33	273.15	54.94
34	280.35	58.41
35	287.50	62.02
36	294.57	65.76
37	301.57	69.63
38	308.49	73.64
39	315.33	77.78
40	322.10	82.06
41	328.78	86.46
42	335.37	90.98
43	341.88	95.64
44	347.75	100.00

Circle Center At X = 95.6 ; Y = 433.2 and Radius, 417.8

*** 1.562 ***

Failure Surface Specified By 44 Coordinate Points

Point No.	X-Surf (ft)	Y-Surf (ft)
1	23.33	21.67
2	31.20	20.22
3	39.10	18.92
4	47.02	17.79
5	54.96	16.81
6	62.91	15.99
7	70.89	15.34
8	78.87	14.84
9	86.86	14.50
10	94.86	14.32
11	102.86	14.30
12	110.86	14.44
13	118.85	14.75
14	126.84	15.21
15	134.82	15.83
16	142.78	16.61
17	150.72	17.55
18	158.65	18.65
19	166.55	19.90
20	174.42	21.32
21	182.27	22.89
22	190.08	24.62
23	197.85	26.50
24	205.59	28.54
25	213.28	30.73
26	220.93	33.08
27	228.53	35.58
28	236.08	38.23
29	243.57	41.03
30	251.01	43.98
31	258.38	47.08
32	265.69	50.33
33	272.94	53.72
34	280.12	57.25
35	287.22	60.93
36	294.25	64.75
37	301.20	68.71
38	308.07	72.81
39	314.86	77.04
40	321.56	81.41
41	328.17	85.92
42	334.69	90.55
43	341.12	95.31
44	347.49	100.00

Circle Center At X = 99.8 ; Y = 414.2 and Radius, 399.9

*** 1.566 ***

References:

- Casagrande, A., (1975). "Liquefaction and deformation of sands - A critical review, Proceedings of Fifth pan American conference on soil mechanics and foundation engineering, Buenos Aires, Argentina- harvard soil mechanics series No. 88 - January 1976. Harvard University, Cambridge - Massachusetts.
- Castro G. and Trancosop J. (1989). Effect of 1985 Chilean earthquake on three tailing dam, Fifth Chilean earthquake engineering August 1989.
- Castro G., (1987). On the behavior of soil during earthquake - Liquefaction " Soil Dynamics and Liquefaction ". A.S.Carmark Editor, elsevier.
- Castro G., (1975). Liquefaction and cyclic mobility of saturated sands. Journal of Geotechnical Engineering Division, ASCE 103 (GTE) pp. 551 - 569.
- Ellinson R.D and Cho Y.Y.(1976) " Dynamic design consolidation of loose fine coal refuse". E.D. Appolomia consulting Engineers, Inc.Proceedings of the Ohio river soils seminar, Lexington,Kentucky October 1976.
- Hardin B.V. and Black W.L. (1968). "Vibration Modulus of Normally consolidated clay" ASCE Vol 94 No.SM2 pp.353-369.
- Hsai -yang Fang, "Foundation Engineering Handbook" McGraw Hill Book company.
- Lee. K. L. and Seed H.B.(1978). "Cyclic stress condition ca liquefactionof sand" Journal of Geotechnical Engineering division, ASCE, vol 93
- Makdisi, F.I. and seed, H. B., (1978). Simplified procedure for estimating dam and embankment Earthquake induced deformation. ASCE

Vol. 104, No. G.T.7, 1978 (849 - 867).

Newmark N. M. (1965). "Effects of Earthquakes on dams and embankments" Geotechnique London England vol. 5.

Poulos S. J., Rohinskey E.I. and Keller T.O., (1986). Liquefaction resistance of thickened tailings. Journal of geotechnical Engineering. ASCE Vol. No. 111.pp. 1380 -1394.

Poulos S.J., Castro, G. and France, J. W., (1985). "Liquefaction evaluation procedure". Journal of Geotechnical Engg. ASCE Vol. No. 111, pp. 772 - 792.

Poulos S. J., (1981). "The steady state of deformation". Journal of Geotechnical Engg. ASCE Vol. No. 107 pp 553 -562

Seed H. B. Schnabel B. and Lysmer J. (1972). " SHAKE : A personal computer based program for earthquake response analysis of horizontally layered soil".

Seed H. B. and Lee. K. L. (1966). "Liquefaction of saturated sand during cyclic loading" Journal of Soil Mechanics and Foundation Divisions ASCE Vol. 92 pp 105-134

Seed H. B. (1979). " Soil liquefaction and cyclic mobility evaluation for level round during eartquakes" Journal of Geotechnical Engineering Division. ASCE Vol. 105 GT2 1979 pp.201-205.

Seigel (1975) Boutroup (1977). "PCSTABL5 :A personal computer based prrogram to determine the embankment stability".

Vick S.G. 1990 , " Planning design and Analysis of Tailings Dams", Bitech publishers Ltd. Vancouver B. C. Canada.

Wasan M. (1995). "Assesment of Liquefaction Potential of Fly Ash Tailings by Steady State Method, Thesis submitted for the award of M. of Technology degree at Indian Institute Of Technology Kanpur".